Examining the Impact of Shallow Groundwater on Evapotranspiration from Uncultivated Land in Colorado's Lower Arkansas River Valley

Brandon M. Lehman
Niklas U. Hallberg
Jeffrey D. Niemann
Timothy K. Gates

April 2010

Completion Report No. 214

Colorado Water Institute

Colorado State University

Abstract:

The Lower Arkansas River Valley (LARV) in Southeastern Colorado is an important agricultural region of the state. However, more than a century of intensive irrigation has raised the water table under the area causing agricultural and environmental problems including water logging, soil salinization, and the leaching of salts and selenium into waterways. These issues could be mitigated by improving irrigation practices, lining irrigation canals, installing subsurface drainage systems, and implementing other strategies that lower the water table. A lower water table is expected to increase crop productivity in some areas, and it is also likely to reduce non-beneficial evapotranspiration (ET) from uncultivated lands that are interspersed with the irrigated fields. Various studies suggest that a lower water table tends to result in lower ET rates, but a quantitative analysis is lacking for conditions that are representative of the uncultivated lands in the LARV. The overarching goal of this research is to determine the contribution of groundwater upflux to the total ET for uncultivated areas in the LARV and to quantify the dependence of ET on water table depth as well as other site properties. Three field sites in the LARV were selected for detailed study. One site is a retired field near the Arkansas River that has a shallow water table due to nearby irrigation. The second site is a naturally vegetated area at the edge of the alluvial valley that has a shallow water table due to its proximity to an irrigation canal. The third site is another naturally vegetated field that lies between an irrigation canal and a creek. These sites are mainly vegetated by grasses and forbs. ET was estimated at a 30 m × 30 m resolution from Landsat satellite imagery using the Remote Sensing of Evapotranspiration (ReSET) method. This method also produces estimates of the Normalized Difference Vegetation Index (NDVI), which is a measure of vegetation greenness, at the same resolution. Water table depths were measured at a total of 84 monitoring wells divided between the three sites. Other variables were measured in the field including precipitation, gravimetric soil moisture, and soil salinity. Clear relationships between ET and water table depth at one of the sites suggest that ET rates decrease with deeper water tables, but ET rates can remain high even when the water table is relatively deep (greater than 2 m). Water balance analyses indicate that groundwater upflux contributes between 80% and 86% of the total ET at these sites. Further study is needed to quantify the water savings that might be achievable for the region as a whole if the water table was lowered through engineering intervention.

Keywords:
Water table, upflux, evaporation, transpiration, remote sensing, Rocky Ford, Southeastern Colorado, irrigated valley, non-beneficial use, losses

Table of Contents

List of Figures

List of Tables

Justification of Work Performed

Many irrigated regions of the world suffer from water logging and salinity problems and the associated negative economic impacts (Wichelns, 1999). The Lower Arkansas River Valley (LARV) in southeastern Colorado (Figure 1) has been extensively irrigated for more than a century, and similar to other agricultural regions around the globe, irrigation has raised the water table in the LARV producing water logging and salinity issues in certain areas. A study between 1999 and 2001 determined that groundwater and soil salinity levels are responsible for an 11-19% reduction in crop productivity in the LARV (Gates et al., 2006) and selenium levels have been found to exceed Colorado Water Quality Control Division standards (Herting and Gates, 2006).

Several methods are being investigated for reducing water tables in order to mitigate current salinity, selenium and water-logging conditions. These include treating canals with flocculants to reduce seepage losses, installing sub-surface drainage, promoting more efficient irrigation practices, and removing invasive phreatophyte species such as tamarisk. Model simulations have estimated that improved irrigation efficiency and decreased canal seepage can reduce ground water recharge and lower the water table by approximately 0.8 m with an associated 20-40% reduction in salt loads to the Arkansas River (Burkhalter and Gates, 2006). Efforts to reduce ground water recharge are expected to not only result in a lower water table under cultivated fields but also under uncultivated land. One 62 km section (50,600 ha) of the LARV was estimated to be 50% uncultivated throughout the growing season of 2003, and upflux from groundwater (G) under this uncultivated land was estimated to be approximately $65 \cdot 10^6$ m^3 per year during a 1999-2001 study (Burkhalter and Gates, 2005). Thus, evapotranspiration (ET) from uncultivated lands is a significant component of the valley's overall water budget.

The effect that a lower water table would have on ET from the uncultivated land remains poorly understood. Various studies have sought to determine the relationship between ET and depth to the water table (D_{wt}) for various regions. For example, Nichols (1994) examined the relationship between transpiration from phreatophyte shrubs and D_{wt} for seven sites in the Great Basin of Nevada and found an exponential decline in the transpiration rate as D_{wt} increases. Nichols (2000) studied the relationship between G and D_{wt} in the same environment. A linear relationship was observed, and D_{wt}, which ranged from 0 to 3.2 m, described approximately 50% of the variation in G. A similar study of ET from phreatophytes in Colorado's San Luis Valley found that a water table drawdown from an average depth of 0.92 m to 2.50 m decreased ET 32% and ET from groundwater 62% (Cooper et al., 2006). This same report and a follow-up study (Sanderson and Cooper, 2008) both concluded that predicted reductions in G are prone to significant error if vegetation changes are not considered. For example, Sanderson and Cooper (2008) reported that total annual G reduced by 26% for a water table decline from 0.13 m to 0.95 m. This result is in contrast to reductions of 39-55% expected from previous studies (Emery, 1973; Emery, 1991; Huntley, 1979).

Theoretical models and physical experiments have also been pursued in this research area. Young et al. (2007) investigated the relationship between bare soil evaporation and D_{wt} using a MOD-HMS model and found an exponential relationship between evaporation and D_{wt}. That research relied only on irrigated, bare soil lysimeter data and therefore the effect of vegetation on the upflux was not considered. Torres and Hanks (1989) developed a lysimeter experiment using spring wheat and two soils (silty clay loam and fine sandy loam) to examine the impact of D_{wt} on ET. Irrigation was applied in order to prevent soil water from dropping below 50% plant available water. Torres and Hanks (1989) found that groundwater under the silty clay loam contributed 90, 41, and 7% to ET for water table depths of 0.5, 1.0, and 1.5 m, respectively, and

92, 31, 9% for fine sandy loam. While this study included vegetation, it did not consider non-irrigated, natural vegetation.

Vegetation characteristics have an important impact on ET. Nichols (2000) concluded that variations in vegetation, in particular plant cover, explained a significant percentage of the variations in ET from groundwater (in fact, more than D_{wt}). Nichols (2000) also showed a strong relationship between D_{wt} and the percentage of canopy cover. Other researchers have found that the normalized difference vegetation index (NDVI) is a good predictor of ET from grasslands (Kondoh and Higuchi, 2001). NDVI is a commonly-used indicator to ascertain various vegetation attributes including plant biomass, green leaf area, and the fraction of absorbed photosynthetically active radiation (Asrar et al., 1984; Tucker, 1979). Kondoh and Higuchi (2001) calculated ET from an energy balance equation using the eddy correlation method, while NDVI was acquired through satellite imagery. They determined that ET rates increase linearly with increases in NDVI. They also found that the relationship differs between the growing season and mature season, suggesting the phenological stage of the grasses influences the relationship between ET and NDVI. More recently, researchers have developed functions using NDVI from satellite imagery to predict annual ET from groundwater (Groeneveld et al., 2007). Groenveld et al. (2007) found that by using a variation of NDVI and local meteorological data, one can predict G in areas supported by shallow water tables with a coefficient of determination of 0.94. One of the characteristics of this study was that water tables were deeper than the limit for capillary rise.

The primary objective of the present research study is to gain a greater understanding of the relationship between ET and a shallow water table for uncultivated lands in the LARV. This study differs from those in the literature because the soil is neither bare (Young et al., 2007) nor exclusively occupied by phreatophytes (Cooper et al., 2006; Nichols, 1994; Nichols, 2000; Sanderson and Cooper, 2008) nor occupied by irrigated crops (Torres and Hanks, 1989). Specific objectives of the project include: (1) determining the variables that are most important in controlling ET rates from uncultivated lands in the LARV with shallow water tables, (2) characterizing the dependence of ET on D_{wt} for these same conditions, and (3) calculating the portion of ET that is attributable to groundwater upflux. The following section (Section 2) describes the data collection methods including the remote sensing methodology used to estimate ET and the field monitoring used to measure potential explanatory variables including D_{wt}. Section 3 analyzes the data in accordance with the project objectives, and Section 4 summarizes the main conclusions and recommendations.
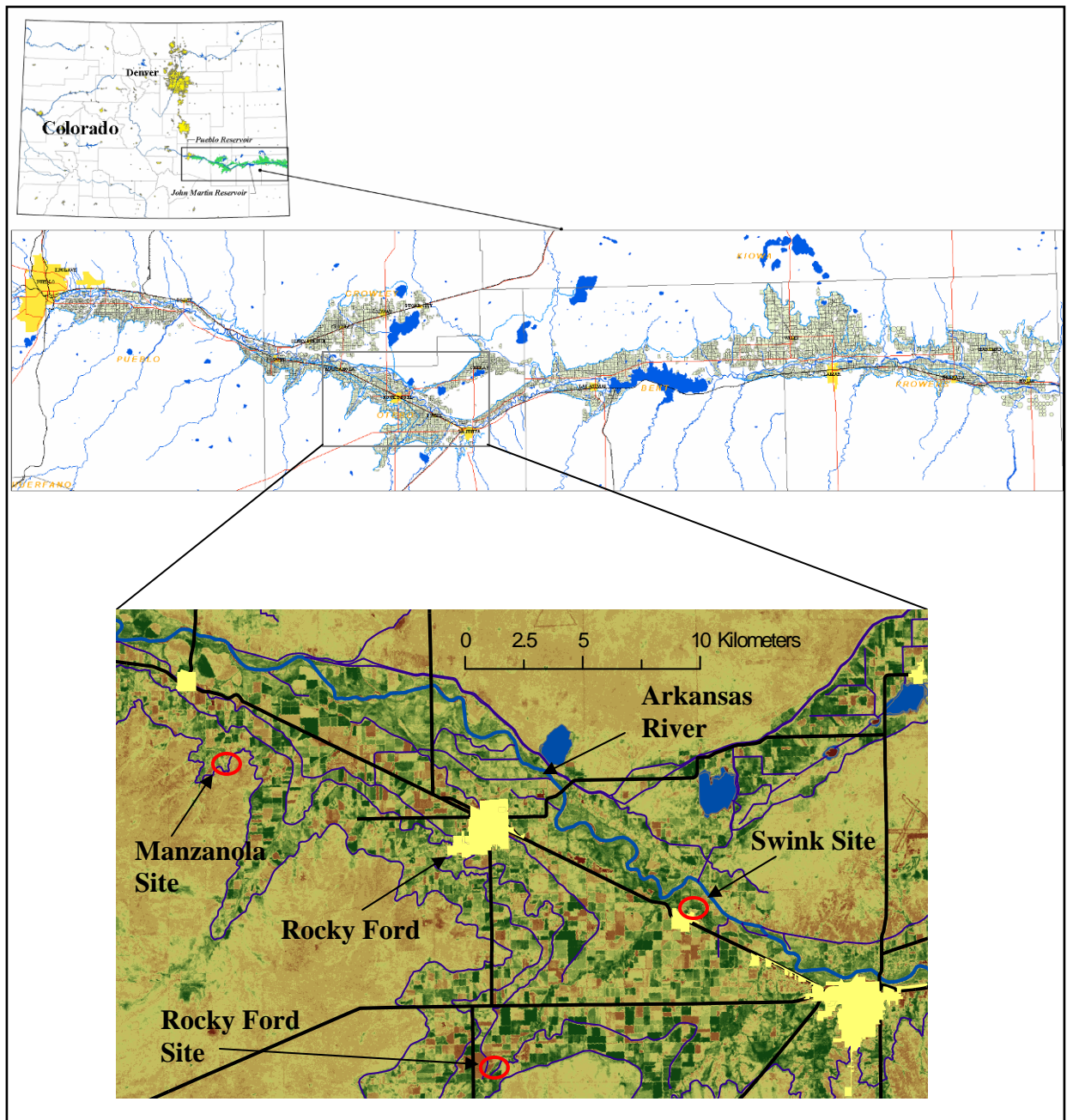
FIGURE 1. *Location of the LARV in southeastern Colorado. The three study sites are identified by red circles in the lowest part of the figure. Black lines are roads, yellow filled areas are towns, blue filled areas are water bodies, and blue lines are rivers and canals.*

Review of Methods Used

The general strategy for this research was to study three uncultivated sites with relatively shallow water tables in the LARV. Actual ET was estimated from a remote sensing method (Elhaddad and Garcia, 2008) that provides spatial patterns of actual ET on particular dates based on satellite images. Water table depths were measured using numerous monitoring wells. Other relevant variables were measured in the field on dates when satellite images were available. The period of study (4/28/07 through 2/28/09) encompasses two irrigation seasons in the LARV, which typically run from the middle of March through the middle of November.

Study Sites and Well Locations

The three study sites lie within the alluvial valley created by the Arkansas River. The field sites are all located within 10 km of Rocky Ford, but each site is named after the nearest town. The Manzanola site is located 4 km southeast of the town of Manzanola, the Swink site is 0.75 km north of the town of Swink, and the Rocky Ford site is 9 km south of Rocky Ford (Figure 1). The Manzanola site is located adjacent to and down slope of the Rocky Ford Highline Canal. The site is approximately 5.1 ha and has 7.8 m of topographic relief. The site is naturally-vegetated and dominated by prairie grasses in low areas with xeric plants, such as yucca and cacti, in areas with higher elevations. Photos of the Manzanola site are shown in Figure 2. The Swink site lies approximately 0.75 km south of the Arkansas River. The site is approximately 13.7 ha and has 1.8 m of topographic relief. It is composed of 3 retired fields and lies adjacent to irrigated alfalfa fields to the south and west. This site used to be an alfalfa field and grazing pasture but is now designated as a conservation easement (some grazing continues on a portion of the site). The southernmost section of the Swink site is dominated by alfalfa which used to be cultivated, a middle portion is grass-dominated but not grazed, and the northern portion is an actively grazed, grass pasture for cattle. Photos of the three distinct portions of the Swink site are shown in Figure 3. The Rocky Ford site lies adjacent to and between the Catlin Canal and Timpas Creek. The site is approximately 3.4 ha and has 1.2 m of topographic relief. The site is naturally-vegetated and dominated by prairie grasses. Photos of the site are shown in Figure 4.
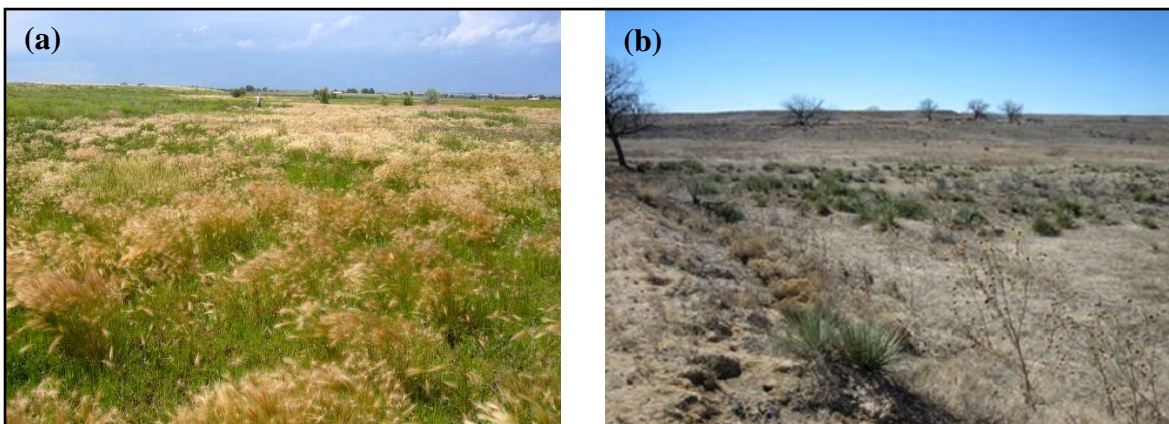
FIGURE 2. *Photos of the Manzanola site (a) looking north from south end of site in early summer and (b) looking southwest from northeast edge of site in late winter.*
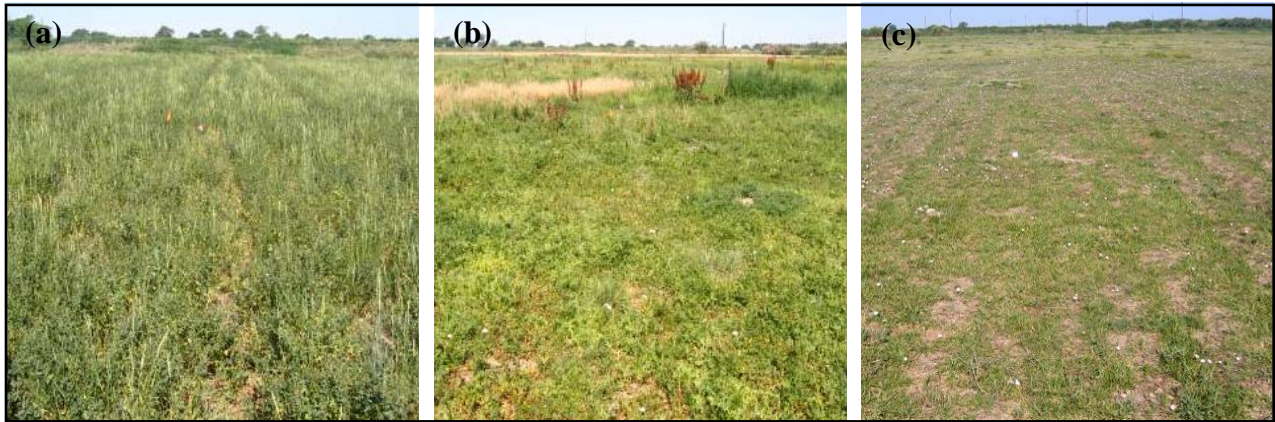
FIGURE 3. *Photos of the Swink site showing (a) the southernmost section, which is dominated by legacy alfalfa, (b) the middle portion, which is dominated by ungrazed grasses, and (c) the northern portion, which is dominated by grazed grasses. All photos are looking east from the west end of site.*
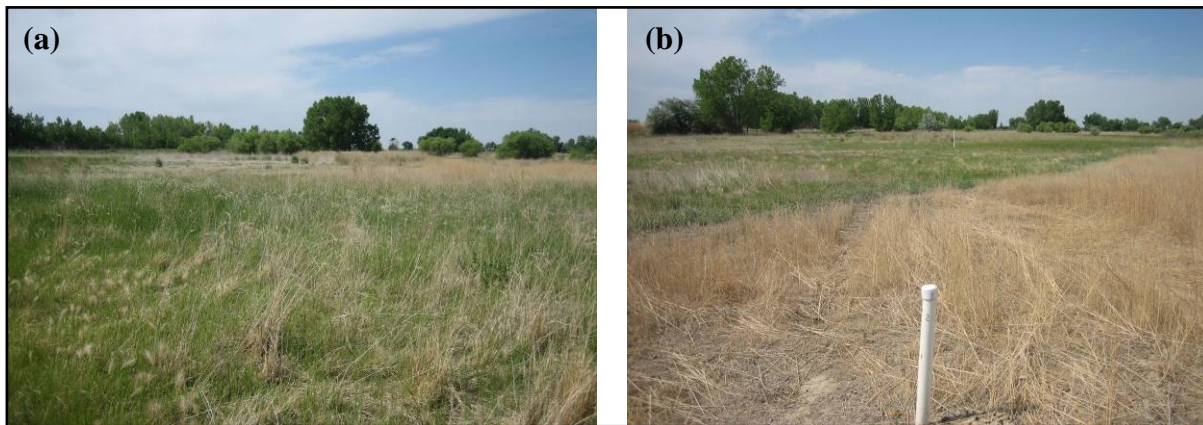
FIGURE 4. *Photos of the Rocky Ford site: (a) looking north from south end of site (trees line Timpas Creek in the background) and (b) looking south from north end of site (trees are near the Catlin Canal in the background).*

Numerous monitoring wells were drilled at each study site to measure D_{wt}, and their locations are shown in Figure 5. The locations of the wells were distributed approximately uniformly at each site, but the typical spacing of the wells varies due to differences in the overall sizes of the sites. At the Manzanola site, 28 monitoring wells were installed on an irregular grid with a spacing of about 45 m. At the Swink site, 39 wells were installed on a grid with a spacing of about 60 m. As shown in the figure, the two southernmost rows of wells were drilled in the section with legacy alfalfa, the third, fourth, and fifth rows from the south were drilled in the ungrazed grass section, and the northernmost row of wells was drilled in the grazed grass section. At the Rocky Ford site, 17 wells were installed with a spacing of about 45 m. Once drilled, the exact location and elevation of each well was determined using a survey-quality global positioning system. The date when groundwater monitoring began at each well is indicated by the markers in Figure 5. Monitoring began at most Manzanola and Swink wells in late April 2007 and continued until late February 2008. Several wells were added to the Manzanola and Swink sites after monitoring began. The Rocky Ford site was monitored only between June and September 2008.
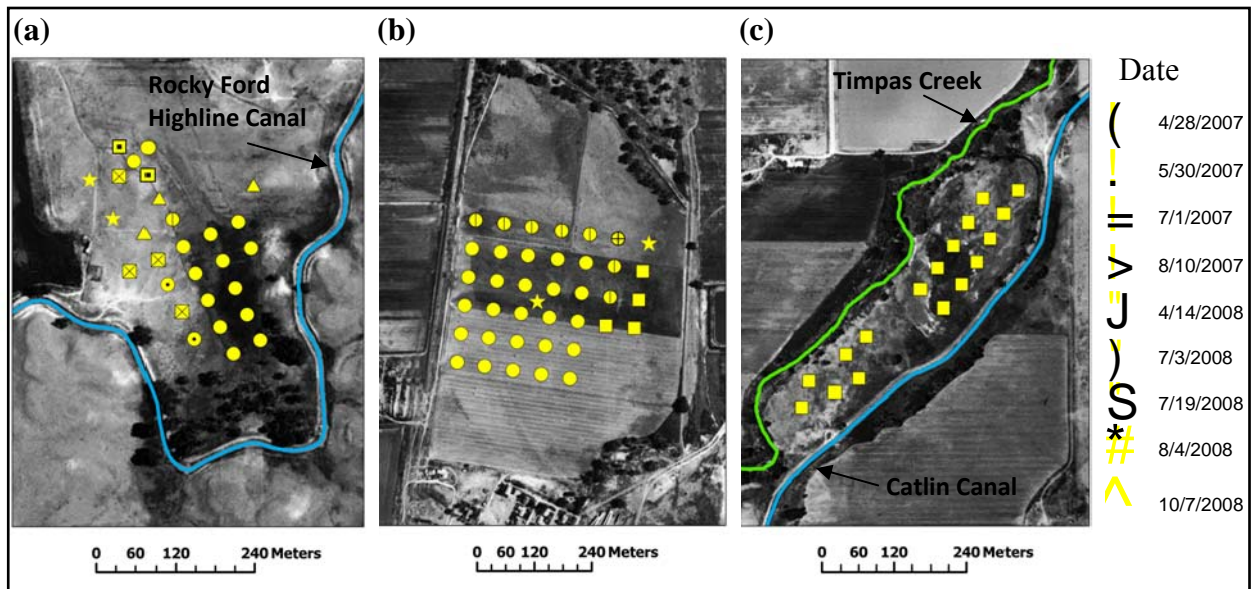
FIGURE 5. *Locations of the monitoring wells superimposed on aerial photos of the (a) Manzanola, (b) Swink and (c) Rocky Ford sites. Dates associated with symbols refer to the date that well monitoring began.*

Estimation of ET

Daily ET (ET_a) on specific dates was estimated using the Remote Sensing of Evapotranspiration (ReSET) method (Elhaddad and Garcia, 2008). This method utilizes either Landsat 5 or Landsat 7 satellite imagery to calculate the surface energy balance and ultimately estimate ET. The Landsat satellites provide multispectral images including the visible (bands 1-3), infrared (bands 4, 5, and 7), and thermal (band 6) ranges of spectrum. Resolutions for the visible and near-infrared bands are 30 m × 30 m, whereas the thermal bands have 120 m × 120 m and 60 m × 60 m resolutions for Landsat 5 and Landsat 7, respectively. Each satellite provides images of the study region every 16 days, but the cycles of the two satellites are offset by 8 days.

The energy balance of the land surface can be written:

$$R_n \ = \ L\rho_w E_i \ + H \ + \ G_o \tag{1}$$

where R_n is the net radiation, L is the latent heat of vaporization, ρ_w is the density of water, E_i is the instantaneous evapotranspiration rate, H is the sensible heat flux, and G_o is the heat conduction to the ground. Using a function developed by Bastiaanssen (2000), R_n is computed from the surface albedo, NDVI, surface temperature, digital elevation models, and surface roughness. The surface albedo is calculated from the visible bands (1, 2, and 3) and infrared bands (4, 5, and 7), NDVI is calculated from bands 3 and 4, and surface temperature is calculated from band 6. G_o is computed using NDVI, albedo, surface temperature, and the sensible heat flux. H is calculated through a process of selecting a "wet" pixel, where water evaporates at the atmospheric requirement, which implies H is zero, and a "dry" pixel, where ET is assumed to be zero, so $H = R_n - G_o$. With the wet and dry H values known, the value for H at other pixels in the image can then be determined.

The latent heat flux ($L\rho_w E_i$) can be calculated once R_n, G_o, and H have been estimated (Bastiaanssen et al., 1998). With the quantity $L\rho_w E_i$ known, the instantaneous evaporative fraction (Λ) can be calculated from the following equation,

$$\Lambda = \frac{L\rho_w E_i}{L\rho_w E_i + H} = \frac{L\rho_w E_i}{R_n - G_o} \tag{2}$$

The Λ values are then converted to a 24 hour actual ET estimate (ET_a) through the following equation, which assumes that the evaporative fraction is constant throughout the day,

$$ET_a = \frac{86,400\Lambda(R_{n24} - G_{0,24})}{L\rho_w} \tag{3}$$

R_{n24} is the 24 hour net radiation (calculation of which is described by Duffie and Beckman (1991)), $G_{o,24}$ is the 24 hour soil heat flux, which is assumed to be zero, and 86,400 is the time conversion from one second to 24 hours.

ReSET was implemented to process Landsat 5 images for 18 dates: 4/28/07, 6/15/07, 7/1/07, 7/17/07, 8/18/07, 9/3/07, 10/5/07, 2/2/08, 2/18/08, 3/21/08, 4/14/08, 4/30/08, 7/3/08, 7/19/08, 8/4/08, 10/7/08, 11/8/08, and 2/28/09. In October 2007, Landsat 5 encountered technical difficulties and was not able to provide imagery, so Landsat 7 images were used instead. Unfortunately, Landsat 7 images have sections with no data in the images due to technical problems with the satellite. These sections affected portions of each field site on certain dates, so analysis of these portions was not possible. Landsat 7 images were processed for 6 dates: 8/10/2007, 9/27/07, 10/29/07, 2/2/08, 2/18/08, and 3/21/08. Ultimately, the ReSET method produces patterns of ET_a at a 30 m × 30 m resolution on each date with an available image. Previous research suggests that these ET estimates have errors on the order of 15% (Elhaddad and Garcia, 2008).

Patterns of ET_a for each field site based on Landsat 5 images from 8/4/2008 and 10/5/2007 are shown in Figure 6. As can be seen in the figure, the monitoring wells used to collect D_{wt} data, do not necessarily fall at the center of a pixel. To obtain an ET_a value at any particular well, an inverse distance interpolation was performed on the ET_a grids from ReSET. The inverse of the squared distance from the selected well to the center of each pixel is used to calculate the weight of that pixel's ET value in a weighted average. Only the ET_a values from cells within a 30 m radius of the selected point were used in the method, which ensures that the ET_a estimates are only based on the neighboring grid cells. The interpolation method was used to generate a new grid at a 0.5 m resolution, and the value of the pixel containing the well was then used as the ET_a value for that well. It should be noted that satellite images can only be georectified with a precision equal to their spatial resolution. In addition, the ET_a values from ReSET are spatial averages within each pixel. Thus, even if the ReSET algorithm could produce perfect estimates of ET_a, the values of ET_a at the wells are expected to include some error.

The patterns of ET_a in Figure 6 are typical for the three sites. The southern end of the Manzanola site usually has greater ET_a values. At the Swink site, the highest ET_a values tend to occur in the alfalfa section of the site, while the lowest values tend to occur in the grazed grass portion of the field. Also, ET_a tends to increase moving from west to east. At the Rocky Ford site, the lowest ET_a values occur at the most southern and northern wells, while the highest ET_a values occur at the central wells. Overall, ET_a is usually greatest at the Swink site followed by the Rocky Ford and Manzanola sites where ET_a is more variable.
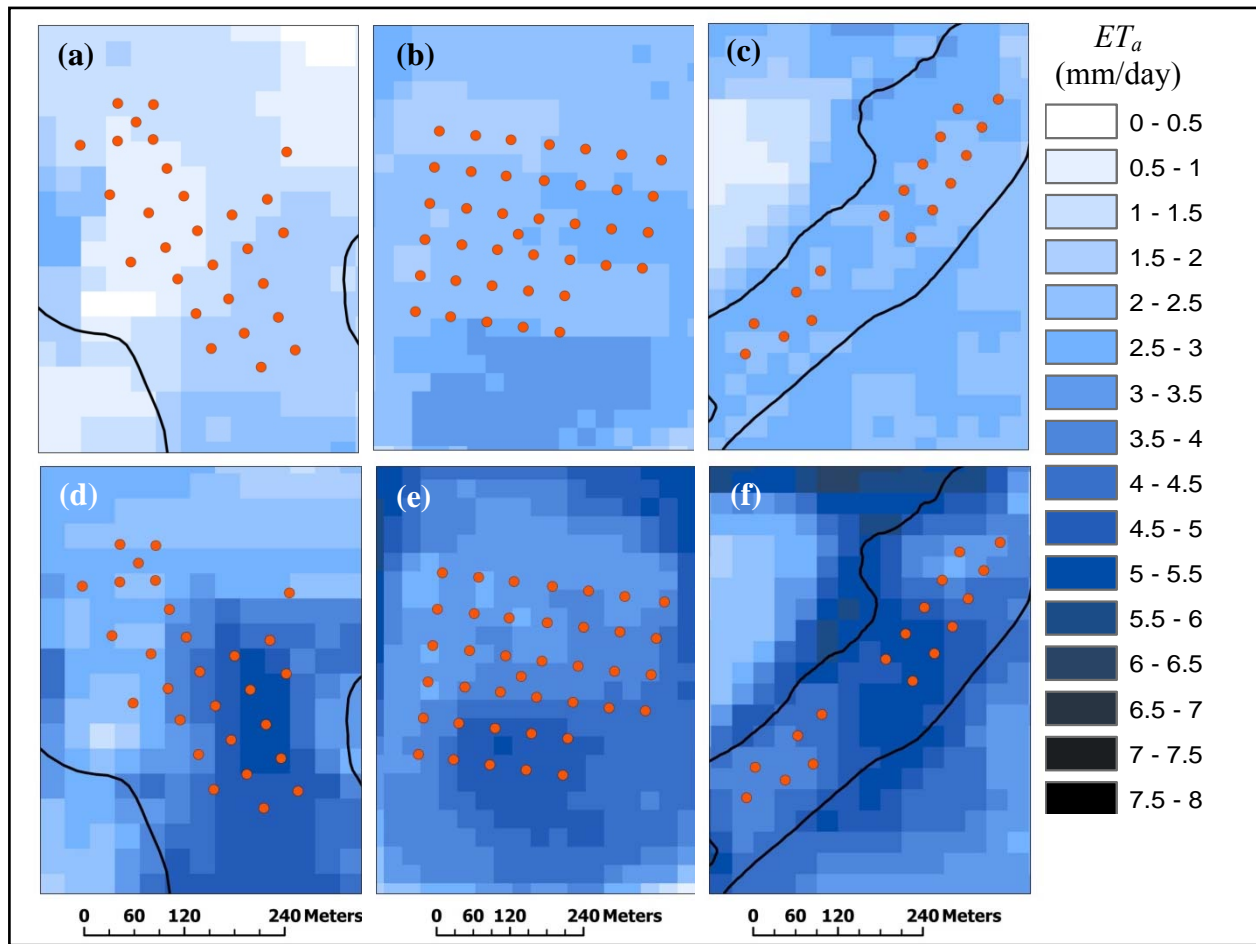
FIGURE 6. *Spatial patterns of ET_a calculated with ReSET for the (a,d) Manzanola, (b,e) Swink and (c,f) Rocky Ford sites. The top row of images (a,b,c) shows the patterns for 10/5/2007, and the bottom row of images (d,e,f) shows patterns for 8/4/2008.*

Measurement of Potential Explanatory Variables

Variables that potentially explain the spatial and temporal variations of ET_a were collected from available sources and/or measured in the field. Water table depths were measured at the monitoring wells using two methods. Manual readings of water table depths were collected with an electric tape in each well on dates when the satellite passed. Pressure transducers (Hobo® Water Level Loggers) were submerged in multiple wells at each field site to record absolute pressure at the depth of the transducer. An additional pressure transducer was used to measure atmospheric pressure at each field site. With absolute pressures known for the atmosphere and at each submerged transducer, water table depths could be calculated at a one hour interval throughout the study period. The transducer-measured water table depths agree closely with hand-measured water table depths. The manual readings are used in all quantitative analyses below because they are available at all wells.

Meteorological variables were obtained from onsite measurements and a nearby weather station. Precipitation was measured using two Davis Instruments Rain Collector II tipping-bucket rain gauges at each field site, which measure 0.254 mm increments of rainfall. The gauges were located in separate open areas at each site approximately 1.25 m above the ground. Reference ET (ET_o) for each day during the study period was calculated using data from a Colorado Agricultural Meteorological Network (CoAgMet) station located at the Arkansas Valley Research Center on the eastern edge of Rocky Ford (Colorado Climate Center, 2008).

The Manzanola, Swink, and Rocky Ford sites are located 14.1, 6.6, and 9.1 km from the CoAgMet station, respectively. ET_o was calculated using the Penman-Monteith method as implemented in the spreadsheet of Snyder and Eching (2002) for a 0.12 m tall reference grass.

A gravimetric soil moisture measurement was taken near each well being monitored for most Landsat dates. An Oakfield probe was used to collect soil samples over a 0-0.30 m depth. Typical samples were 100-200 g. Due to the quantity of soil samples collected and limited access to an oven, soil samples were dried for a minimum of two weeks in a greenhouse and a regression equation for each field was used to convert the water content estimated from the greenhouse-dried soil samples (WC_g) to an oven-dried equivalent (WC_o). The regression equations were developed by drying a subset of the greenhouse-dried samples in an oven at 105 °C for 24 hours and then weighing the samples again (Pikul, 2008). Samples less than 75 g wet weight were not used to develop the regression equation in order to reduce the effect of measurement error. Samples used in the regression include 182 and 113 measurements from the Manzanola and Swink sites, respectively. The data and regression equations are shown in Figure 7 along with the coefficient of determination (r^2). The figures confirm that the water content estimated from greenhouse drying is highly correlated with the water content estimated from oven drying, particularly at the Manzanola site where a wider range of water contents were available. Equivalent oven-dried water contents were not calculated for the Rocky Ford site because this field was not included in any analysis requiring water content.
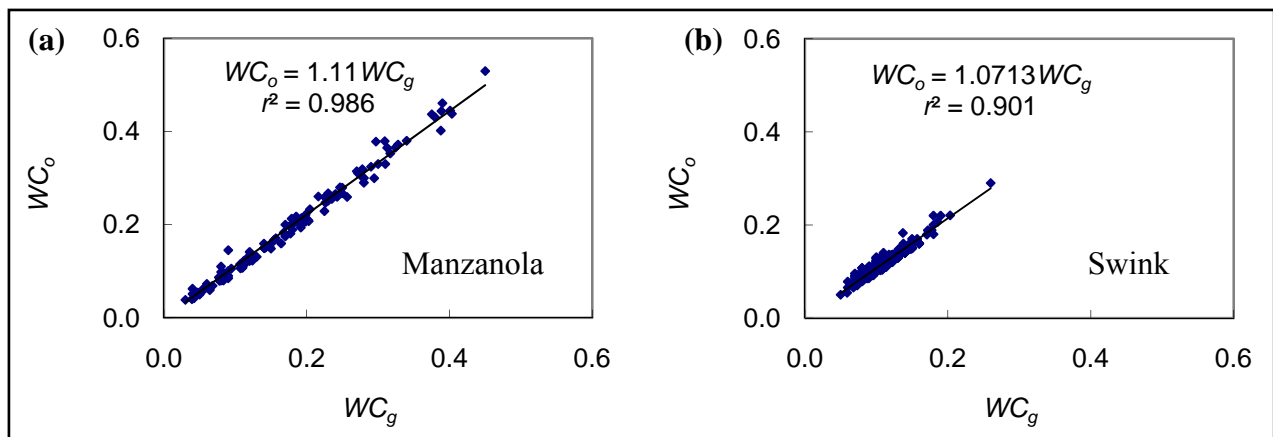
FIGURE 7. *Plots comparing gravimetric soil water content determined from greenhouse drying (WC_g) and oven drying (WC_o) for the (a) Manzanola and (b) Swink sites along with the associated regression equations.*

Soil water salinity was characterized using the electrical conductivity of a soil paste extract (EC_e) in dS/m, which was estimated for each well based on measurements obtained within one day of each satellite date. A Geonics EM-38 was used to take electromagnetic measurements in the vertical direction (EM_v), up to 1.5 m, in order to reach the root zone. Recent research calibrated EM-38 readings to EC_e values in the LARV (Wittler et al., 2006). In this method, the EM_v data are first adjusted for soil temperature by multiplying each EM_v value by the following factor:

$$f_{tc} = 1.8509 - 0.0516951(T) + 0.000858442(T^2) - 0.00000613535(T^3) \qquad (4)$$

where T (°C) is the average soil temperature determined from measurements between the ground surface and a depth of 1.22 m at 0.30 m increments. EC_e (dS/m) is then determined using the following equation:

$$EC_e = 0.45 + 7.23EM_v^{1.78} + 19.54WC_g - 34.06EM_v(WC_g) \qquad (5)$$

where WC_g is the average greenhouse-dried gravimetric soil moisture determined from measurements between the ground surface and a depth of 1.22 m at 0.30 m increments. Due to time limitations, it is typically not feasible to collect soil moisture and temperature profile data at every EM_v measurement location. Thus, five soil moisture/temperature profiles were averaged by Wittler et al. (2006) and used to obtain EC_e values in a given field. A similar approach was used in this analysis. The Manzanola and Rocky Ford sites each contained two regions with relatively distinct soil moisture values. Therefore, each site was divided into two sections, one having the water table within 1.22 m and the other having the water table below 1.22 m. Two soil moisture and temperature profiles were used to calculate averages for each section at the Manzanola and Rocky Ford Sites. Four profiles were averaged for the entire Swink site.

Rather than using a single EM_v measurement to calculate EC_e for each well, measurements were taken at each well and at a specified distance in the cardinal directions of the well grid at each site. A distance of 15 m was used at both the Manzanola and Rocky Ford sites, while 30 m was used at the Swink site. The five EM_v measurements were used to produce five EC_e values, which were then averaged to produce a single EC_e value for each well.

NDVI is calculated from the digital number of band 3 (red) and band 4 (NIR) as follows:

$$NDVI = \frac{NIR - red}{NIR + red} \qquad (6)$$

NDVI can theoretically range from -1 to 1, but it typically ranges from 0.2 to 0.8 for real vegetated surfaces. Studies show strong relationships between NDVI and leaf area index (LAI) for grasslands and vegetation cover with LAI values up to two (Gamon et al., 1995). NDVI values were calculated at a 30 m resolution from each Landsat image and then interpolated to each well using the same inverse distance weighted algorithm as was used for ET_a. Spatial patterns of NDVI calculated from Landsat 5 images on 10/5/07 and 8/4/08 are shown in Figure 8. NDVI is typically greatest at the Swink site with the Manzanola site showing the most spatial variation.
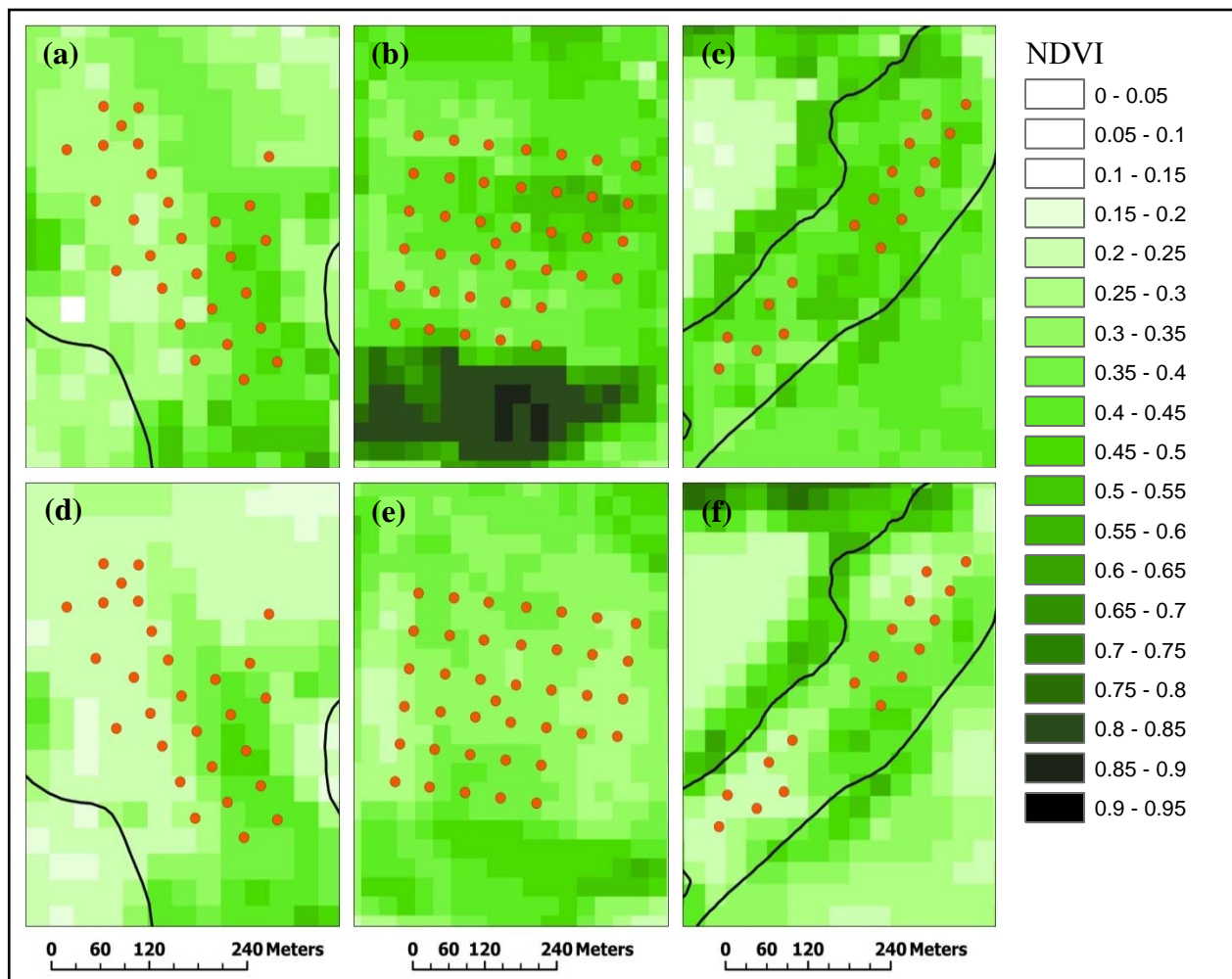
FIGURE 8. *Spatial patterns of NDVI at the (a,d) Manzanola, (b,e) Swink and (c,f) Rocky Ford sites. (a,b,c) show the patterns for 10/5/200, and (d,e,f) show the patterns for 8/4/2008.*

Soil texture can play an important role in water movement through the soil profile and can therefore affect many hydrologic processes including ET. A single soil sample was collected adjacent to each well that was installed prior to July 19, 2008 with an Oakfield probe to a depth of 0.30 m. The samples were then analyzed using a standard hydrometer method (Gavlak et al., 2003). Soil texture results for the three study sites are shown in Figure 9. One can see that the soil texture at the Manzanola site is coarser than that of the Swink site and much coarser than that of the Rocky Ford site. Soil textures plotted on the USDA Soil Classification Triangle are shown in Figure 10. The soils at the Manzanola site generally fall in the clay loam and loam classifications. The soils at the Swink site are relatively variable, ranging from silty clay to loam. In contrast, the soils at the Rocky Ford site have little variability, ranging from silty clay to silty clay loam.
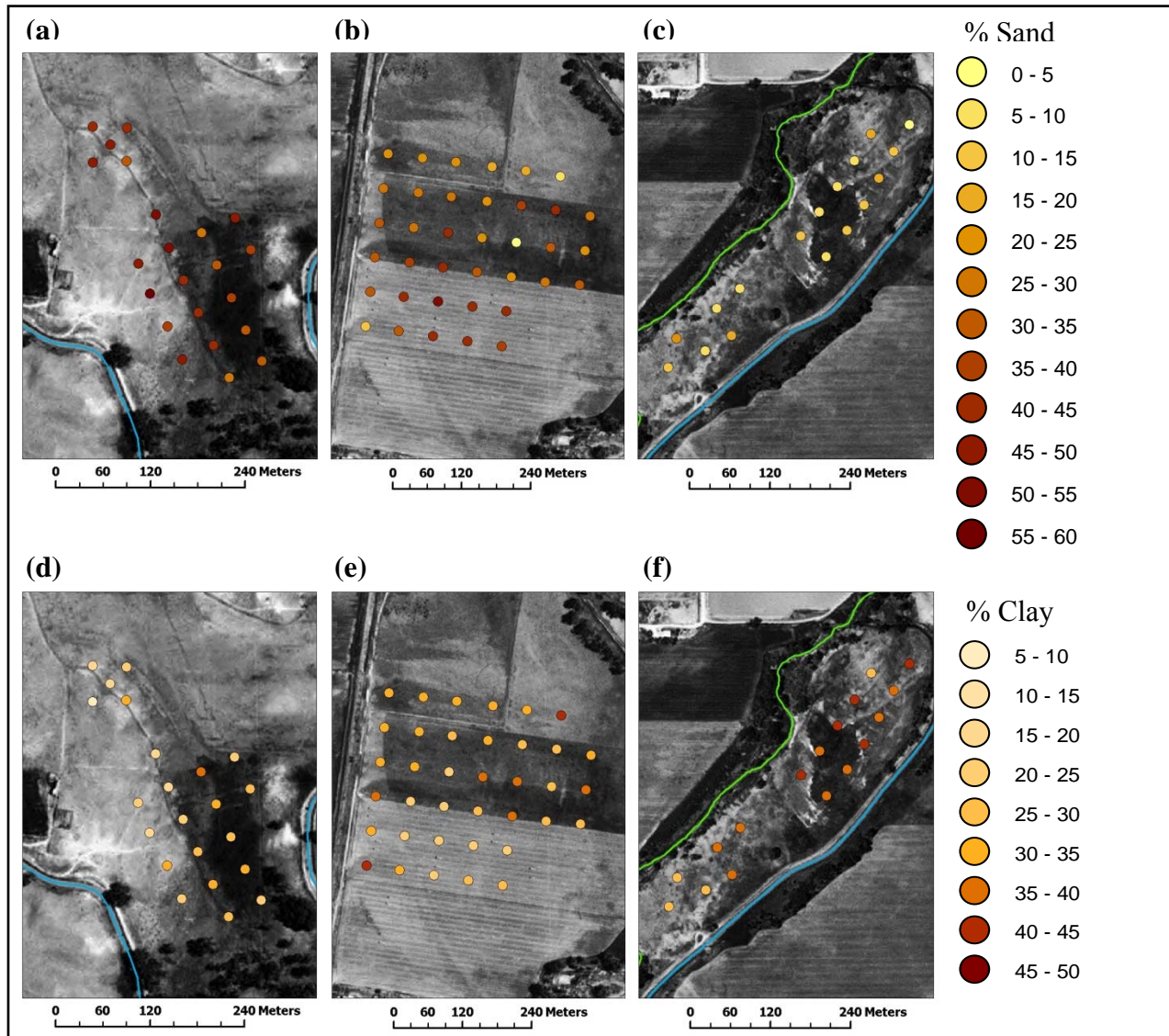
FIGURE 9. *Percent sand and clay at the (a,d) Manzanola, (b,e) Swink and (c,f) Rocky Ford sites.*
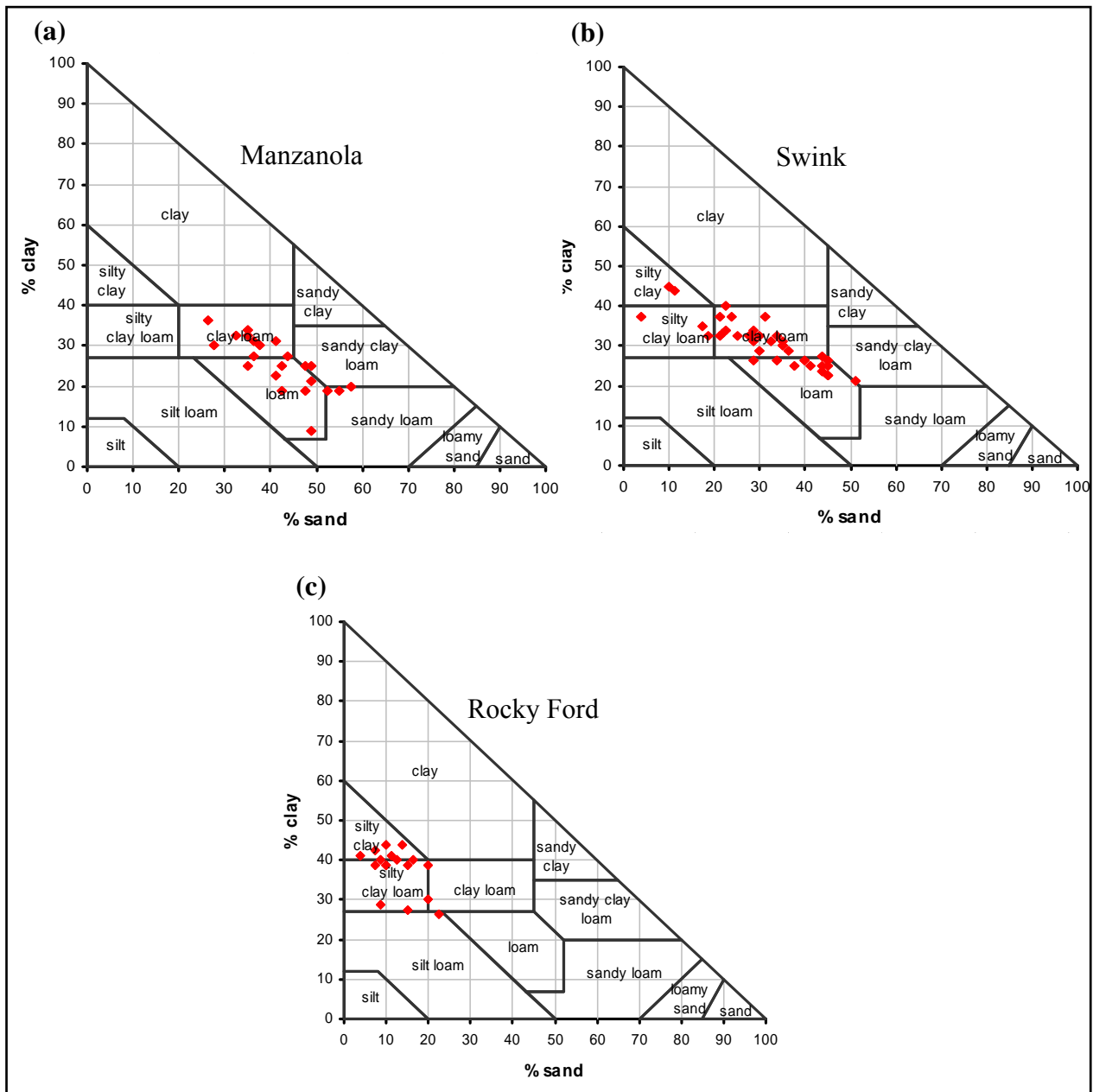
FIGURE 10. *Soil texture classifications for samples taken at the (a) Manzanola, (b) Swink, and (c) Rocky Ford sites plotted on the USDA Soil Classification Triangle. Figure was generated using software from Gerakis and Baer (1999).*

Discussion of Results

Basic Hydrologic Behavior of Field Sites

The daily precipitation, water table depth, and ET_o for the study period (4/21/07 to 2/28/09) at the Manzanola and Swink sites are shown in Figure 11. The Rocky Ford Site is not shown due to its short period of observation. Note that ET_o is the same in both plots because the same CoAgMet station is used to represent both sites. Total precipitation measured during the study period was 0.57 m at Manzanola and 0.43 m at Swink. Total CoAgMet ET_o was 2.63 m. The dashed vertical lines indicate the dates for which both Landsat images and field data are available. The water table depths shown in the figure are from representative wells that have complete records for the observation period. Two water table depths are shown for the Manzanola site because this site has two sections with rather distinct water table depths. The shallow water table is measured at the easternmost well of the southernmost row of 3 wells; it ranges from 0 to 1.5 m. The deeper water table is measured at the westernmost monitoring well of the two northernmost wells at the site; it ranges from about 0.9 to 2.5 m. The water table measurements at the Swink site are taken from the monitoring well that is third from the west in the fifth row from the south. The water table ranges from about 1.0 to 1.7 m. When considering all monitoring wells throughout the study period, the water table depth at the Manzanola site varies significantly in space and time, ranging from 0 m to 6.4 m. During the growing season, the water table is relatively stable, but it drops steadily after mid November until early April. This behavior is likely due to the operation of the Rocky Ford Highline Canal, which flows full between March 15 and November 15. The water table depth at the Swink site is more stable, ranging from approximately 0.8 m to 2.6 m. Fluctuations are most likely due to precipitation events as well as pumping and irrigation activities at nearby fields.

Factors Most Associated with Space-Time ET Variations

In this section, we determine how much of the space-time variations in ET_a can be explained by the available site characteristics. We begin by exploring the strength of the relationship between the ET_a and ET_o. Note that ET_o is the same at all locations where ET_a is estimated because ET_o was determined from a single weather station. Thus, ET_o can only explain variations in ET_a between different days in the dataset. ET_o depends on various meteorological variables including air temperature, solar radiation, and wind speed (Allen et al., 1998). Wind speed in particular can vary significantly between individual days, and these fluctuations are expected to be relatively localized within the LARV. Thus, wind speeds observed at the CoAgMet station may not be representative of conditions at the field sites. In addition, the vegetation may be unable to adjust to rapid fluctuations in ET_o. To reduce the effect of such fluctuations, an average ET_o is calculated by averaging over a specified number of days.

Table 1 shows the r^2 values between ET_a and ET_o. In this table, ET_o is determined by averaging the value on the date on which ET_a is observed and the values from up to 6 preceding days (labeled $ET_{o,1...7}$). The table shows the r^2 values when the ET_a data are limited to the Manzanola site, the Swink site, or include both sites. When either site is considered alone, the 2-day average ET_o is most closely associated with the ET_a values, and this result also holds when all the data is grouped together. The 2-day average ET_o
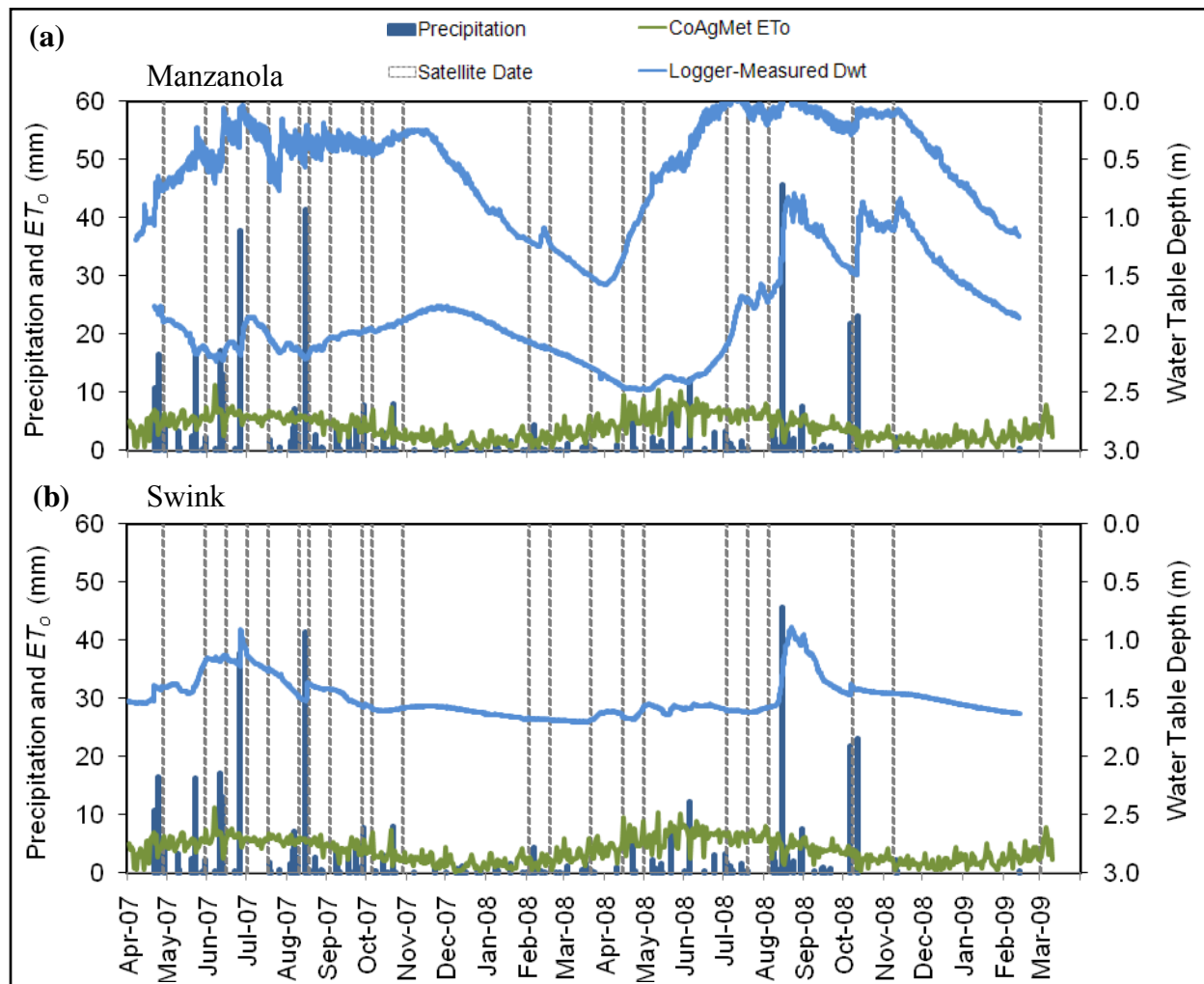
FIGURE 11. *Daily precipitation, CoAgMet ET$_o$, and transducer-measured water table depths for the (a) Manzanola and (b) Swink sites. A transducer-measured water table depth is plotted for the two distinct sections found at the Manzanola site and a representative location at the Swink site.*

TABLE 1. *r2 values for calculated between ETa and ETo,1…7 for the Manzanola, Swink, and combined datasets as labeled in table.*

	ETo, 1	ETo, 2	ETo, 3	ETo, 4	ETo, 5	ETo, 6	ETo, 7
Manzanola	0.15	0.30	0.20	0.20	0.17	0.19	0.19
Swink	0.45	0.54	0.47	0.49	0.47	0.48	0.49
Combined	0.36	0.47	0.39	0.40	0.38	0.39	0.40

In order to determine whether site characteristics such as D_{wt} can explain additional variation in ET_a, an empirical model is hypothesized. This model has a multiplicative structure because such a structure has been frequently used to model ET in the literature (Albertson and Kiely, 2001; Allen et al., 1998; Teuling and Troch, 2005). The general form of the model is:

$$\hat{ET}_a = \alpha\beta\gamma\delta ET_o \tag{7}$$

where $\hat{ET}_a$ is the estimated ET and α, β, γ, and δ are functions that describe the influences of vegetation (α), soil moisture (β), groundwater (γ), and salinity (δ) on ET. ET_o is the reference ET averaged over a specified period. Our general strategy is to first propose possible functions

for α, β, γ, and δ based on the literature. Next, the parameters in those functions will be calibrated to minimize the disagreement between the observed ET values and those estimated by Equation (7) when each function is used. We can then determine which functions (i.e. α, β, γ, and/or δ) and which specific forms of those functions are most successful at explaining the variability of ET_a.

The following functions are considered to describe the impact of vegetation on ET_a:

$$\alpha_1 = 1 - \exp\left\{-a_1\left[a_2 - (1-a_2)\sin\left(2\pi\frac{DOY-a_3}{365}+\frac{\pi}{2}\right)\right]\right\} \tag{8}$$

$$\alpha_2 = a_4\,\text{NDVI} + a_5 \tag{9}$$

$$\alpha_3 = a_6 T_{soil} + a_7 \tag{10}$$

where $a_1...a_7$ are parameters that must be calibrated, DOY is the Julian day of the year, and T_{soil} is the daily minimum soil temperature measured at a 5 cm depth (available from the CoAgMet data). T_{soil} and DOY were included as potential explanatory variables because research has shown that they affect plant growth (Nakano et al., In Press; Yan and Wallace, 1998). NDVI is related to the vegetation density and greenness as discussed earlier.

The following functions are considered to describe the influence of soil moisture availability:

$$\beta_1 = \left(\frac{WC_g}{b_1}\right)^{b_2} \tag{11}$$

$$\beta_2 = \begin{cases} WC_g / b_3 & \text{if } 0 \le WC_g \le b_3 \\ 1 & \text{if } b_3 \le WC_g \le 1 \end{cases} \tag{12}$$

$$\beta_3 = \begin{cases} 0 & \text{if } WC_g < b_4 \\ \dfrac{WC_g - b_4}{b_5 - b_4} & \text{if } b_4 \le WC_g \le b_5 \\ 1 & \text{if } WC_g > b_5 \end{cases} \tag{13}$$

$$\beta_4 = \begin{cases} 0 & \text{if } WC_g < b_7 \\ b_6\,\dfrac{WC_g - b_7}{b_8 - b_7} & \text{if } b_7 \le WC_g \le b_8 \\ b_9 + (1 - b_9)\dfrac{WC_g - b_8}{b_{10} - b_8} & \text{if } b_8 \le WC_g \le b_{10} \\ 1 & \text{if } WC_g > b_{10} \end{cases} \tag{14}$$

where WC_g is the gravimetric soil moisture in the top 0.30 m of the soil and $b_1...b_{10}$ are parameters that must be calibrated. Equation (11) describes the reduction in ET_a that occurs when moisture is limited with a power function of WC_g. Equation (12) implies that the ET becomes progressively limited by moisture availability once the gravimetric moisture is below a threshold (b_3). Equation (13) includes the same effect but implies that ET completely ceases below another threshold (b_4). Equation (14) includes a threshold where the vegetation becomes stressed and transpiration ceases (b_8) and another threshold where both evaporation and transpiration cease (b_7).

16

The following functions are considered to describe the impact of groundwater proximity on ET:

$$\gamma_1 = g_1 D_{wt} + g_2 \tag{15}$$

$$\gamma_2 = g_3 / D_{wt}^{\ g_4} \tag{16}$$

$$\gamma_3 = g_5 / (D_{wt} - g_6)^{g_7} \tag{17}$$

$$\gamma_4 = g_8 \exp(-g_9 D_{wt}^{\ g_{10}}) \tag{18}$$

where $g_1 ... g_{10}$ are parameters that must be calibrated. Equation (15) is a linear function and was suggested as a possible relationship between ET and D_{wt} by Nichols (2000). Equation (16) is an exponential function, which is similar to one found by Sanderson and Cooper (2008) in their research. Equation (17) is comparable to a function found by Gowing et al. (2006), and Equation (18) is much like a function that Nichols (1994) used to relate D_{wt} and G.

Only a single function is considered to describe the effects of soil salinity:

$$\delta = d_1 EC_e + d_2 \tag{19}$$

where d_1 and d_2 are coefficients that must be calibrated.

For simplicity, we begin by calculating regression statistics for the model in Equation (7) when only a single function (α, β, γ, or δ) is multiplied by $ET_{o,1...7}$. The parameters for each function were found using an optimization method to maximize r^2. It should be noted that there is no guarantee that a global optimum is found by the optimization method. Also, it is expected that functions with more parameters will typically perform better because they are more flexible. However, it is also possible that the flexibility allowed in a particular function is not useful.

Tables 2 through 4 show r^2 values for models based on data from the Manzanola site, the Swink site, and both the Manzanola and Swink sites combined. The Rocky Ford site is not included in this analysis because it has relatively little data. By including local characteristics, the r^2 values are typically much higher than those observed earlier when only ET_o was included (Table 1). For the Manzanola site, the highest r^2 value (0.81) is found when using α_2 (which depends on NDVI) and a 2 to 4-day average ET_o. Similarly, the highest r^2 value (0.81) for the Swink data is found when using α_2 and a 4-day average ET_o. Similar results are also observed when the Manzanola and Swink data are combined. It should be noted that NDVI is used by ReSET to estimate ET_a. Thus, the dependence observed here is not surprising. However, it should be noted that α_1 or α_3 can be used in place α_2 and the r^2 values are still reasonably high. In fact, after α_2, α_1 (which depends on DOY) is the next best function for the Swink data and the combined data, while β_1 (power function of soil moisture) is the next best function for the Manzanola data.

It is also interesting to note that most of the proposed functions perform reasonably well. Among the β functions, β_1 and β_4 perform much better than β_2 and β_3 with β_1 performing the best. β_2 and β_3 perform nearly identically because β_3 can become identical to β_2 when particular values are chosen for its parameters. Among the γ functions, γ_1 and γ_4 slightly outperform γ_3, while γ_2 performs the worst for the Manzanola data and the combined data. All γ functions give nearly identical results for the Swink site. Although variations in vegetation-related characteristics are most associated with variation in ET_a, variations in water table depth are also relatively successful at explaining ET_a. Based on these data, however, one cannot conclusively determine which model for the dependence on D_{wt} is best (although γ_2, the exponential model, seems slightly inferior to the others).

17

Next, the model in Equation (7) was applied by considering every combination of two functions (e.g., $\alpha\beta$, $\alpha\gamma$, $\alpha\delta$, $\beta\gamma$, etc.). Note that only one function out of a particular group (α, β, γ, or δ) was allowed in any given application of Equation (7), so a model with $\alpha_1\alpha_2$ was not considered, for example. Models containing two functions and $ET_{o,1...7}$ perform only slightly better than those containing a single function, so these results are not shown in detail. The small difference suggests that the variations in the vegetation, soil moisture, groundwater, and salinity characteristics are probably correlated among themselves. The better a particular function performs when considered alone, the smaller the observed increase in r^2 when it is paired with an additional function. For the Manzanola data, the best models, in decreasing order of r^2, contain α_2, α_1, β_1, β_4, γ_1, γ_4, or γ_3 and a second function. The remaining combinations have similar, lower values of r^2. For the Swink data, the best models, in decreasing order of r^2, contain an α_2 or α_1 and a second function. When considering the combined data, the best models, in decreasing order of r^2, contain α_2, α_1, or β_4 and another function.

Regression analysis performed using 3 and 4 functions in Equation (7) give very small increases in r^2 over the 1 and 2 function versions. Increases when adding additional functions are only on the order of hundredths. Overall, including 1 function in Equation (7) appears to be adequate.

TABLE 2. *r^2 values for models constructed by multiplying a single α, β, γ, or δ and $ET_{o,1...7}$ as labeled in the table using only data from the Manzanola site.*

	α_1	α_2	α_3	β_1	β_2	β_3	β_4	γ_1	γ_2	γ_3	γ_4	δ
ETo, 1	0.67	0.73	0.62	0.69	0.46	0.46	0.68	0.68	0.65	0.67	0.68	0.63
ETo, 2	0.73	0.81	0.69	0.77	0.59	0.59	0.75	0.76	0.72	0.75	0.76	0.70
ETo, 3	0.71	0.81	0.66	0.76	0.55	0.55	0.74	0.74	0.70	0.73	0.74	0.67
ETo, 4	0.72	0.81	0.67	0.77	0.55	0.55	0.74	0.75	0.71	0.74	0.75	0.68
ETo, 5	0.71	0.79	0.66	0.75	0.53	0.53	0.72	0.73	0.69	0.73	0.74	0.66
ETo, 6	0.70	0.77	0.65	0.73	0.53	0.53	0.71	0.72	0.68	0.71	0.72	0.65
ETo, 7	0.71	0.77	0.66	0.73	0.52	0.52	0.71	0.73	0.68	0.72	0.73	0.66

TABLE 3. r^2 values for models constructed by multiplying a single α, β, γ, or δ and $ET_{o,1...7}$ as labeled in the table using only data from the Swink site.

	α_1	α_2	α_3	β_1	β_2	β_3	β_4	γ_1	γ_2	γ_3	γ_4	δ
ETo, 1	0.69	0.75	0.63	0.64	0.59	0.59	0.65	0.64	0.64	0.64	0.64	0.63
ETo, 2	0.72	0.80	0.68	0.70	0.66	0.66	0.70	0.69	0.69	0.69	0.69	0.68
ETo, 3	0.70	0.79	0.65	0.67	0.63	0.63	0.67	0.65	0.65	0.65	0.65	0.65
ETo, 4	0.72	0.81	0.67	0.68	0.64	0.64	0.68	0.67	0.67	0.67	0.67	0.66
ETo, 5	0.71	0.79	0.65	0.66	0.61	0.61	0.66	0.65	0.65	0.65	0.65	0.65
ETo, 6	0.70	0.77	0.65	0.65	0.60	0.60	0.65	0.64	0.64	0.64	0.64	0.64
ETo, 7	0.72	0.78	0.67	0.66	0.60	0.60	0.66	0.66	0.66	0.66	0.66	0.66

TABLE 4. r^2 values for empirical models constructed by multiplying a single α, β, γ, or δ and $ET_{o,1...7}$ as labeled in the table using data from the Manzanola and Swink study sites.

	α_1	α_2	α_3	β_1	β_2	β_3	β_4	γ_1	γ_2	γ_3	γ_4	δ
ETo, 1	0.68	0.74	0.63	0.65	0.55	0.55	0.65	0.64	0.63	0.64	0.64	0.62
ETo, 2	0.73	0.80	0.68	0.71	0.64	0.64	0.71	0.70	0.69	0.70	0.70	0.68
ETo, 3	0.70	0.79	0.65	0.69	0.61	0.61	0.69	0.67	0.66	0.67	0.68	0.65
ETo, 4	0.72	0.80	0.67	0.70	0.62	0.62	0.70	0.69	0.67	0.68	0.69	0.66
ETo, 5	0.70	0.78	0.65	0.68	0.60	0.60	0.68	0.67	0.65	0.66	0.67	0.64
ETo, 6	0.70	0.77	0.65	0.67	0.58	0.58	0.67	0.66	0.64	0.65	0.66	0.63
ETo, 7	0.72	0.77	0.66	0.68	0.58	0.58	0.68	0.67	0.65	0.67	0.68	0.65

Spatial Variations of ET, Water Table Depth, and NDVI

The spatial variability of ET_a and its associations with D_{wt} and NDVI were explored by analyzing the data after it is averaged through time at each well. Figure 12 plots the average ET_a against the average D_{wt} for each well. The dates used to calculate the averages are consistent for all wells and are listed in the figure. It is clear from Figures 12a and 12b that the relationship between the average ET_a and D_{wt} is much stronger at the Manzanola site than at the Swink site. Because the Swink site has three sections with relatively distinct vegetation types (legacy alfalfa, grass, and grazed grass), Figures 12d, 12e, and 12f divide the Swink data according to these sections. Some of the wells in each section are close enough to the edge of their section that the associated ET_a values may represent a mixture of vegetation types. Thus, only a single, unaffected row of wells was included for each section in the figures (the 2nd, 4th, and 6th rows when counting from south to north in Figure 5b). When divided in this way, visually stronger relationships are observed, especially for the alfalfa and grass sections. However, the number of data points in each case becomes quite small. Overall, these results suggest that the vegetation type affects the relationships between ET_a and D_{wt}, but for a given vegetation type, average ET_a decreases as average D_{wt} becomes large. It is also clear that the average ET_a remains relatively large even when the average D_{wt} is relatively large (greater than 2 m).

Figure 13 plots the relationships between average NDVI and D_{wt} in the same manner. Here again, stronger relationships are observed between average NDVI and D_{wt} at the Manzanola site than at the Swink site as whole. However, the relationships at the Swink site become stronger when the site is divided between the three vegetation types as described earlier. These results indicate that the density and greenness of the vegetation as captured in NDVI is associated with variations in the average D_{wt}.

Table 5 shows the results of linear regressions between average ET_a and D_{wt}, average NDVI and D_{wt}, and average ET_a and NDVI. The table contains the slopes of the regression lines, the p-values, and the r^2 statistics. The table shows that the average ET_a is more correlated with the average NDVI than the average D_{wt}. However, the correlations in both cases are statistically significant except for the relationship between ET_a and D_{wt} when all the Manzanola data is combined. This result is expected because the previous section showed similar behavior for the individual ET_a values. Table 5 also confirms that the correlation between NDVI and D_{wt} is statistically significant in most cases. Together these results indicate that spatial variations in NDVI are most important in explaining spatial variations in ET_a. However, spatial variations of NDVI are often closely related to variations in D_{wt}. The results also suggest that human activities such as grazing and planting crops can obscure these dependencies.

Regressions between soil texture characteristics and the average ET_a, D_{wt}, and NDVI were also performed. ET_a and NDVI are positively correlated with percent clay at the Manzanola site, while they are negatively correlated with percent clay at the Swink site. D_{wt} is positively correlated with percent sand and negatively correlated to percent silt and percent clay at both fields. Overall, the relationships are much stronger at the Manzanola site.
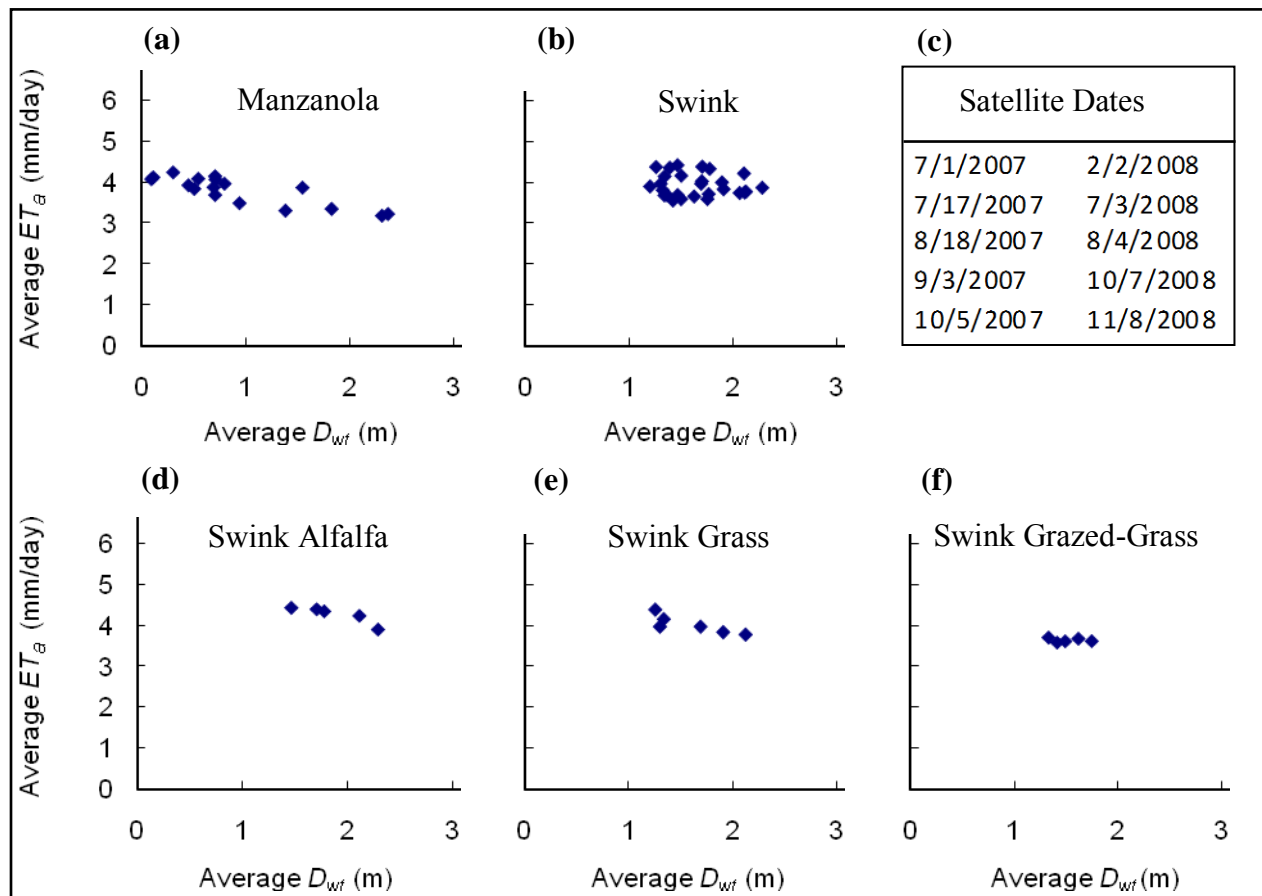
FIGURE 12. *Average ET_a plotted against average water table depth for the (a) Manzanola site and (b) Swink site. Plots (d, e, f) for the alfalfa, grass, and grazed grass sections of the Swink site, respectively. Dates used to generate the averages are shown in (c).*
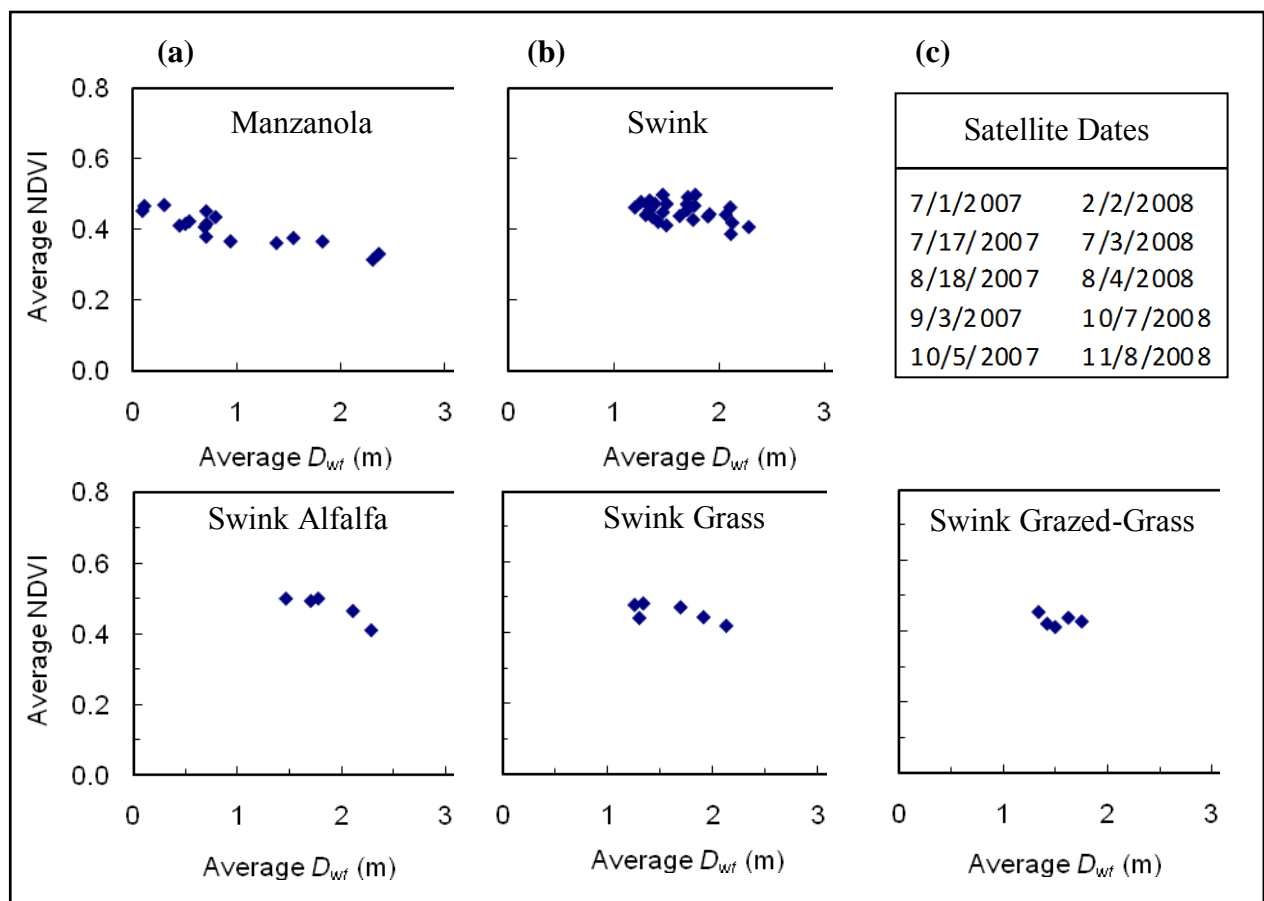
FIGURE 13. *Average NDVI plotted against average water table depth for the (a) Manzanola site and (b) Swink site. Plots (d, e, f) for the alfalfa, grass, and grazed grass sections of the Swink site, respectively. Dates used to generate the averages are shown in (c).*

TABLE 5. *Linear regression results for the temporally averaged data shown in Figures 12 and 13. Significant (<0.05) p-values are shown in bold.*

	$ET_a : D_{wt}$			$NDVI : D_{wt}$			$ET_a : NDVI$			
	Slope	r^2	p-Value	Slope	r^2	p-Value	Slope	r^2	p-Value	No. of Wells
Manzanola	-0.43	0.73	**1.2E-05**	-0.058	0.79	**1.7E-06**	7.3	0.88	**3.2E-08**	17
Swink	-0.093	0.01	6.0E-01	-0.039	0.18	**2.7E-02**	7.2	0.55	**9.0E-06**	27
Swink Alfalfa	-0.61	0.82	**3.5E-02**	-0.11	0.80	**4.2E-02**	5.6	0.97	**2.3E-03**	5
Swink Grass	-0.50	0.69	**4.1E-02**	-0.048	0.49	1.2E-01	7.2	0.67	**4.7E-02**	6
Swink Grazed-Grass	-0.065	0.04	7.4E-01	-0.027	0.07	6.6E-01	2.8	0.78	**4.5E-02**	5

Linear regression results between ET_a and D_{wt}, NDVI and D_{wt}, and ET_a and NDVI for each individual date are shown in Tables 6-11. Results for the Manzanola, Swink, and Rocky Ford sites are shown in Tables 6, 7, and 8, respectively. Tables 9, 10, and 11 contain results from the alfalfa, grass, and grazed-grass rows in the Swink site.

The tables show that ET_a is correlated with D_{wt} and NDVI for the Manzanola and Rocky Ford sites on nearly all dates. Aside from 3 dates in the late winter/early spring of 2008, the correlations between ET_a and D_{wt} are significant and the sign of the slope of the regression equation is less than zero for the Manzanola data. In addition, with the exception of 2 additional dates in the spring of 2008, the correlations between NDVI and D_{wt} are all significant with slopes less than zero. The average r^2 values for all dates are 0.49, 0.49, and 0.59 for linear regressions between ET_a and D_{wt}, NDVI and D_{wt}, and ET_a and NDVI, respectively (again for Manzanola). The three dates analyzed for the Rocky Ford site show similar behavior.

21

Less than one fourth of the dates analyzed at the Swink site produced significant regressions for the relationship between ET_a and D_{wt} and even fewer dates for the relationship between NDVI and D_{wt}. Correlations between ET_a and NDVI are usually significant at the site. The average r^2 values for all dates are 0.10, 0.07, and 0.52 for linear regressions between ET_a and D_{wt}, NDVI and D_{wt}, and ET_a and NDVI, respectively. When dividing the data between the three sections with different vegetation, the fraction of dates with significant correlations increases but not by much due to the small number of data points. The average r^2 values are 0.68, 0.54, and 0.67 for linear regressions between ET_a and D_{wt}, NDVI and D_{wt}, and ET_a and NDVI, respectively for the alfalfa section. Similarly, they are 0.57, 0.39, 0.54 for the grass section, and 0.50, 0.40, and 0.55 for the grazed-grass section. The r^2 value from 10/29/07 was not included in the average for the grazed-grass section because only 2 wells were available on that date (so r^2 is necessarily 1).

Regressions between soil texture characteristics and ET_a, D_{wt}, and NDVI for each day were also performed. For the Manzanola site, relatively strong relationships were observed between both percent clay and percent sand and all three variables. The relationships at the Swink site were relatively weak. At the Rocky Ford site, percent clay is negatively correlated with D_{wt}.

TABLE 6. *Linear regression results for ET_a and NDVI as a function of D_{wt} and ET_a as a function of NDVI for the Manzanola site. Significant (<0.05) p-values are shown in bold.*

	$ET_a : D_{wt}$			$NDVI : D_{wt}$			$ET_a : NDVI$			
Date	Slope	r^2	p-Value	Slope	r^2	p-Value	Slope	r^2	p-Value	No. of Wells
4/28/07	-0.31	0.34	**3.0E-02**	-0.023	0.06	4.2E-01	3.70	0.44	**9.4E-03**	14
5/30/07	-0.39	0.41	**7.7E-03**	-0.053	0.50	**2.2E-03**	5.93	0.55	**1.1E-03**	16
6/15/07	-0.31	0.37	**1.2E-02**	-0.078	0.62	**3.0E-04**	4.20	0.66	**1.2E-04**	16
7/1/07	-0.22	0.40	**6.4E-03**	-0.034	0.38	**7.9E-03**	4.91	0.58	**3.8E-04**	17
7/17/07	-0.57	0.55	**6.5E-04**	-0.038	0.42	**5.2E-03**	9.95	0.60	**2.8E-04**	17
8/10/07	-0.70	0.43	**4.5E-03**	-0.095	0.38	**8.8E-03**	6.83	0.96	**2.8E-12**	17
8/18/07	-0.21	0.18	8.9E-02	-0.046	0.47	**2.4E-03**	6.50	0.77	**3.4E-06**	17
9/3/07	-0.38	0.46	**2.8E-03**	-0.069	0.63	**1.4E-04**	5.36	0.68	**5.1E-05**	17
9/27/07	-0.48	0.60	**7.3E-04**	-0.073	0.68	**1.4E-04**	6.29	0.80	**7.6E-06**	15
10/5/07	-0.35	0.43	**4.2E-03**	-0.077	0.64	**1.3E-04**	4.75	0.71	**2.2E-05**	17
10/29/07	-0.28	0.76	**1.1E-04**	-0.048	0.70	**3.7E-04**	4.77	0.73	**1.8E-04**	13
2/2/08	0.04	0.06	3.4E-01	-0.015	0.06	3.3E-01	1.22	0.18	8.5E-02	17
2/18/08	0.13	0.69	1.7E-01	-0.007	0.42	3.5E-01	-3.00	0.04	7.9E-01	4
3/21/08	1.8	0.01	7.4E-01	-0.010	0.06	4.4E-01	227	0.32	5.7E-02	12
4/14/08	-0.24	0.39	**9.9E-03**	-0.012	0.16	1.3E-01	3.73	0.09	2.5E-01	16
4/30/08	-0.39	0.70	**5.9E-05**	-0.011	0.13	1.8E-01	7.04	0.20	8.3E-02	16
7/3/08	-0.66	0.73	**3.2E-06**	-0.065	0.73	**3.6E-06**	9.13	0.81	**1.3E-07**	19
7/19/08	-0.97	0.76	**5.8E-08**	-0.059	0.73	**2.0E-07**	14.9	0.86	**1.9E-10**	23
8/4/08	-0.62	0.65	**6.3E-07**	-0.049	0.63	**1.4E-06**	11.6	0.86	**1.3E-11**	26
10/7/08	-0.30	0.69	**4.0E-08**	-0.054	0.82	**3.4E-11**	5.31	0.80	**1.8E-10**	28
11/8/08	-0.12	0.75	**3.1E-09**	-0.025	0.78	**4.3E-10**	3.78	0.59	**2.0E-06**	28
2/28/09	-0.12	0.42	**2.4E-04**	-0.013	0.72	**2.5E-08**	9.83	0.69	**7.1E-08**	27

TABLE 7. *Linear regression results for ET_a and NDVI as a function of D_{wt} and ET_a as a function of NDVI for the Swink site. Significant (<0.05) p-values are shown in bold.*

	$ET_a : D_{wt}$			$NDVI : D_{wt}$			$ET_a : NDVI$			
Date	Slope	r^2	p-Value	Slope	r^2	p-Value	Slope	r^2	p-Value	No. of Wells
4/28/07	0.38	0.02	5.5E-01	0.055	0.03	4.1E-01	8.75	0.85	**4.7E-11**	25
5/30/07	0.06	0.00	8.4E-01	-0.033	0.03	4.2E-01	5.75	0.65	**1.2E-06**	25
6/15/07	-1.05	0.22	**1.7E-02**	-0.023	0.01	5.6E-01	9.59	0.67	**5.2E-07**	25
7/1/07	0.22	0.03	3.3E-01	0.037	0.08	1.3E-01	7.10	0.55	**1.3E-06**	32
7/17/07	-0.23	0.01	5.5E-01	0.010	0.00	8.1E-01	8.30	0.81	**4.3E-12**	31
8/10/07	-0.16	0.02	4.3E-01	-0.022	0.03	3.1E-01	7.35	0.66	**9.4E-09**	33
8/18/07	0.35	0.14	**3.1E-02**	-0.020	0.03	3.0E-01	2.02	0.06	1.9E-01	33
9/3/07	-0.29	0.11	5.9E-02	-0.042	0.09	9.3E-02	2.36	0.14	**2.9E-02**	33
9/27/07	-0.28	0.27	**6.0E-03**	-0.074	0.20	**1.8E-02**	2.03	0.36	**8.6E-04**	27
10/5/07	-0.11	0.02	4.9E-01	-0.047	0.07	1.3E-01	2.73	0.29	**1.4E-03**	33
10/29/07	-1.01	0.32	7.0E-02	-0.167	0.54	**1.0E-02**	7.11	0.82	**1.2E-04**	11
2/2/08	0.33	0.29	**1.1E-03**	-0.014	0.05	2.2E-01	4.16	0.20	**9.5E-03**	33
2/18/08	0.13	0.08	1.1E-01	-0.005	0.01	5.5E-01	6.70	0.56	**5.5E-07**	33
3/21/08	0.3	0.03	4.2E-01	-0.014	0.07	2.0E-01	21.0	0.51	**6.8E-05**	25
4/14/08	-0.35	0.03	3.7E-01	-0.034	0.06	1.8E-01	14.1	0.88	**1.3E-15**	33
4/30/08	0.64	0.04	2.5E-01	0.058	0.05	1.9E-01	10.9	0.78	**1.1E-11**	33
7/3/08	-0.13	0.02	4.0E-01	-0.029	0.02	3.8E-01	3.82	0.68	**4.1E-10**	37
7/19/08	-0.83	0.60	**3.4E-05**	0.017	0.09	1.9E-01	-3.09	0.03	4.7E-01	21
8/4/08	-0.19	0.01	5.2E-01	0.003	0.00	8.4E-01	6.07	0.13	**2.8E-02**	37
10/7/08	0.01	0.00	9.4E-01	-0.017	0.01	5.8E-01	1.83	0.72	**2.4E-11**	38
11/8/08	-0.13	0.04	2.3E-01	-0.057	0.09	7.0E-02	2.98	0.80	**1.3E-14**	39
2/28/09	0.03	0.00	8.9E-01	-0.008	0.04	2.3E-01	15.6	0.27	**1.2E-03**	36

TABLE 8. *Linear regression results for ET_a and NDVI as a function of D_{wt} and ET_a as a function of NDVI for the Rocky Ford site. Significant (<0.05) p-values are shown in bold.*

	$ET_a : D_{wt}$			$NDVI : D_{wt}$			$ET_a : NDVI$			
Date	Slope	r^2	p-Value	Slope	r^2	p-Value	Slope	r^2	p-Value	No. of Wells
7/3/08	-0.12	0.52	**1.1E-03**	-0.028	0.75	**6.6E-06**	4.52	0.72	**1.6E-05**	17
7/19/08	-0.39	0.75	**7.4E-06**	-0.037	0.82	**6.8E-07**	9.68	0.78	**2.8E-06**	17
8/4/08	-0.39	0.67	**6.2E-05**	-0.043	0.81	**7.4E-07**	8.67	0.74	**8.8E-06**	17

TABLE 9. *Linear regression results for ET_a and NDVI as a function of D_{wt} and ET_a as a function of NDVI for the alfalfa section at the Swink site. Significant (<0.05) p-values are shown in bold.*

| | $ET_a : D_{wt}$ | | | $NDVI : D_{wt}$ | | | $ET_a : NDVI$ | | | |
Date	Slope	r^2	p-Value	Slope	r^2	p-Value	Slope	r^2	p-Value	No. of Wells
4/28/07	-0.18	0.56	1.5E-01	-0.009	0.03	7.9E-01	1.65	0.15	5.2E-01	5
5/30/07	-0.83	0.75	5.6E-02	-0.226	0.86	**2.3E-02**	3.41	0.76	5.3E-02	5
6/15/07	-2.19	0.84	**2.8E-02**	-0.211	0.82	**3.3E-02**	9.39	0.84	**2.9E-02**	5
7/1/07	-0.72	0.84	**2.9E-02**	-0.067	0.82	**3.3E-02**	10.2	0.93	**7.3E-03**	5
7/17/07	-1.91	0.70	7.6E-02	-0.228	0.51	1.8E-01	6.50	0.83	**3.0E-02**	5
8/10/07	-0.68	0.68	8.5E-02	-0.129	0.52	1.7E-01	4.46	0.95	**4.5E-03**	5
8/18/07	-0.10	0.06	6.9E-01	-0.098	0.65	9.9E-02	1.88	0.30	3.4E-01	5
9/3/07	-0.31	0.81	**3.8E-02**	-0.036	0.73	6.4E-02	7.65	0.88	**1.9E-02**	5
9/27/07	-0.18	0.19	4.7E-01	-0.005	0.05	7.1E-01	12.0	0.41	2.5E-01	5
10/5/07	-0.19	0.45	2.2E-01	-0.037	0.63	1.1E-01	5.33	0.79	**4.3E-02**	5
10/29/07	NA	NA	NA	NA	NA	NA	NA	NA	NA	NA
2/2/08	0.14	0.62	1.1E-01	-0.033	0.58	1.3E-01	-2.11	0.25	3.9E-01	5
2/18/08	0.16	0.67	9.1E-02	-0.001	0.01	8.9E-01	-6.50	0.31	3.3E-01	5
3/21/08	-0.90	0.78	3.1E-01	-0.020	0.67	3.9E-01	41.0	0.98	8.0E-02	3
4/14/08	-0.55	0.98	**8.2E-04**	-0.084	0.95	**5.2E-03**	6.32	0.98	**1.0E-03**	5
4/30/08	-1.15	0.96	**2.9E-03**	-0.156	0.75	5.9E-02	5.95	0.84	**2.9E-02**	5
7/3/08	-1.02	0.93	**8.5E-03**	-0.280	0.99	**3.1E-04**	3.69	0.96	**3.8E-03**	5
7/19/08	NA	NA	NA	NA	NA	NA	NA	NA	NA	NA
8/4/08	-1.39	0.72	6.8E-02	-0.096	0.46	2.1E-01	11.2	0.92	**8.9E-03**	5
10/7/08	-0.08	0.26	3.8E-01	-0.095	0.51	1.8E-01	1.00	0.81	**3.9E-02**	5
11/8/08	-0.16	0.91	**1.2E-02**	0.006	0.02	8.1E-01	-0.97	0.05	7.2E-01	5
2/28/09	-0.28	0.80	**4.1E-02**	-0.012	0.19	4.6E-01	7.57	0.42	2.4E-01	5

TABLE 10. *Linear regression results for ET_a and NDVI as a function of D_{wt} and ET_a as a function of NDVI for the grass section at the Swink site. Significant (<0.05) p-values are shown in bold.*

| | $ET_a : D_{wt}$ | | | $NDVI : D_{wt}$ | | | $ET_a : NDVI$ | | | |
Date	Slope	r^2	p-Value	Slope	r^2	p-Value	Slope	r^2	p-Value	No. of Wells
4/28/07	-0.65	0.40	2.5E-01	-0.127	0.56	1.5E-01	5.88	0.94	**5.8E-03**	5
5/30/07	-0.16	0.19	4.6E-01	-0.027	0.09	6.3E-01	-0.17	0.00	9.5E-01	5
6/15/07	-0.83	0.89	**1.6E-02**	-0.029	0.26	3.8E-01	10.4	0.47	2.0E-01	5
7/1/07	-0.40	0.44	1.5E-01	-0.046	0.29	2.7E-01	4.48	0.41	1.7E-01	6
7/17/07	-1.41	0.77	**2.2E-02**	-0.083	0.55	9.3E-02	13.1	0.84	**1.0E-02**	6
8/10/07	-0.42	0.53	1.0E-01	-0.056	0.67	**4.8E-02**	8.06	0.91	**3.0E-03**	6
8/18/07	-0.09	0.01	8.3E-01	-0.014	0.12	4.9E-01	18.5	0.84	**9.8E-03**	6
9/3/07	-0.68	0.75	**2.6E-02**	0.002	0.00	9.5E-01	-1.10	0.00	9.0E-01	6
9/27/07	-0.30	0.28	2.8E-01	-0.051	0.46	1.4E-01	3.49	0.22	3.5E-01	6
10/5/07	-0.57	0.75	**2.7E-02**	-0.041	0.15	4.5E-01	4.26	0.47	1.3E-01	6
10/29/07	-1.75	1.00	**1.6E-02**	-0.218	1.00	**1.6E-02**	8.00	1.00	**0.0E+00**	3
2/2/08	0.06	0.05	6.7E-01	-0.045	0.66	5.1E-02	0.00	0.00	1.0E+00	6
2/18/08	-0.12	0.05	6.5E-01	-0.020	0.23	3.4E-01	11.1	0.87	**7.0E-03**	6
3/21/08	-0.90	0.45	2.1E-01	-0.030	0.57	1.4E-01	29.0	0.74	6.1E-02	5
4/14/08	-0.96	0.77	**2.1E-02**	-0.062	0.71	**3.6E-02**	14.5	0.97	**4.1E-04**	6
4/30/08	-1.15	0.77	**2.2E-02**	-0.022	0.18	4.0E-01	1.07	0.00	9.4E-01	6
7/3/08	-0.21	0.48	8.6E-02	-0.001	0.00	9.7E-01	1.66	0.24	2.6E-01	7
7/19/08	-0.90	0.96	**9.7E-05**	0.037	0.47	8.8E-02	-11.6	0.45	9.7E-02	7
8/4/08	-0.87	0.85	**2.9E-03**	0.034	0.29	2.2E-01	-6.10	0.17	3.6E-01	7
10/7/08	-0.21	0.62	**3.5E-02**	-0.065	0.34	1.7E-01	1.82	0.58	**4.7E-02**	7
11/8/08	-0.46	0.76	**1.1E-02**	-0.129	0.72	**1.5E-02**	3.45	0.98	**2.8E-05**	7
2/28/09	-0.73	0.81	**1.5E-02**	-0.013	0.29	2.7E-01	27.6	0.67	**4.6E-02**	6

TABLE 11. *Linear regression results for ET_a and NDVI as a function of D_{wt} and ET_a as a function of NDVI for the grazed-grass section at the Swink site. Significant (<0.05) p-values are shown in bold.*

	$ET_a : D_{wt}$			$NDVI : D_{wt}$			$ET_a : NDVI$			
Date	Slope	r^2	p-Value	Slope	r^2	p-Value	Slope	r^2	p-Value	No. of Wells
4/28/07	NA	NA	NA	NA	NA	NA	NA	NA	NA	NA
5/30/07	NA	NA	NA	NA	NA	NA	NA	NA	NA	NA
6/15/07	NA	NA	NA	NA	NA	NA	NA	NA	NA	NA
7/1/07	0.62	0.38	2.7E-01	0.182	0.74	6.0E-02	4.28	0.81	**3.6E-02**	5
7/17/07	0.90	0.66	9.6E-02	0.136	0.45	2.2E-01	5.12	0.88	**1.9E-02**	5
8/10/07	0.42	0.82	**1.3E-02**	0.080	0.69	**4.1E-02**	4.54	0.88	**5.8E-03**	6
8/18/07	0.08	0.01	8.3E-01	0.163	0.60	7.1E-02	2.23	0.46	1.4E-01	6
9/3/07	-0.25	0.46	1.4E-01	0.031	0.19	3.8E-01	-1.93	0.14	4.7E-01	6
9/27/07	NA	NA	NA	NA	NA	NA	NA	NA	NA	NA
10/5/07	0.54	0.49	1.2E-01	0.143	0.36	2.1E-01	2.97	0.85	**8.5E-03**	6
10/29/07	-1.70	1.00	NA	-0.043	1.00	NA	39.0	1.00	NA	2
2/2/08	0.20	0.36	2.1E-01	-0.099	0.68	**4.4E-02**	-1.54	0.31	2.5E-01	6
2/18/08	-0.11	0.15	4.4E-01	-0.043	0.28	2.8E-01	2.74	0.67	**4.8E-02**	6
3/21/08	-0.75	0.53	1.0E-01	-0.064	0.33	2.3E-01	8.95	0.91	**3.4E-03**	6
4/14/08	-1.14	0.76	**2.3E-02**	-0.050	0.44	1.5E-01	15.7	0.82	**1.3E-02**	6
4/30/08	-0.42	0.63	5.8E-02	0.009	0.01	8.7E-01	1.55	0.09	5.7E-01	6
7/3/08	-0.11	0.07	6.1E-01	-0.041	0.15	4.5E-01	3.29	0.69	**4.2E-02**	6
7/19/08	NA	NA	NA	NA	NA	NA	NA	NA	NA	NA
8/4/08	-0.88	0.62	6.2E-02	0.089	0.43	1.6E-01	-1.29	0.02	7.7E-01	6
10/7/08	-0.18	0.54	5.9E-02	-0.009	0.00	8.8E-01	0.35	0.04	6.8E-01	7
11/8/08	-0.60	0.80	**7.0E-03**	-0.261	0.63	**3.4E-02**	1.95	0.92	**5.8E-04**	7
2/28/09	-0.86	0.73	**1.5E-02**	-0.038	0.38	1.4E-01	9.13	0.31	1.9E-01	7

Contribution of Groundwater Upflux to Total ET

In the previous sections, we examined how much of the variability in ET could be attributed to variations in the D_{wt} and other factors. We now evaluate the contribution of groundwater upflux to the total ET by analyzing the water balance of the root zone in each field. The water balance can be written:

$$L\frac{d\theta}{dt} = F - ET + G \tag{24}$$

where L is the thickness of the root zone, θ is the average volumetric soil moisture, F is the infiltration rate, ET is the evapotranspiration rate, and G is the groundwater upflux. Due to the dry conditions at the study sites, lateral flow in the root zone can be safely neglected in the water balance. For the same reason, it is assumed that all precipitation infiltrated into the soil during the study period, so F can be replaced by the precipitation rate P. Using this assumption and a discrete approximation for the derivative, one can solve for G:

$$G = ET - P + L\frac{\Delta\theta}{\Delta t} \tag{25}$$

where $\Delta\theta$ is the change in volumetric soil moisture during a time increment Δt.

To evaluate Equation (25), the depth L was selected to be 0.30 m because the soil moisture samples were collected at this depth. Using this depth essentially neglects changes in soil moisture below 0.30 m. Any changes in this deeper soil moisture are lumped into the

groundwater upflux term in Equation (25). To calculate the ET on every date, an ET efficiency was first calculated on each date with a satellite image as ET_a / ET_o, where ET_o is the reference ET from the CoAgMet station. The ET efficiencies for consecutive satellite dates were then linearly interpolated to get ET efficiencies for each day during the intervening periods. The ET efficiencies were then multiplied by the daily ET_o values from CoAgMet to estimate the actual ET on each day. The precipitation rate was calculated by averaging the measurements from the two rain gages that were placed at each field site (in some periods, one rain gage was not operating reliably so a single gage was used). Field-average soil moisture on each date with a satellite image was calculated by averaging the gravimetric soil water contents from that date and multiplying the average by an assumed bulk density of 0.00139 g/(mm)^3 to obtain a field-average volumetric soil moisture. The bulk density value was originally measured at the Rocky Ford Agricultural Experiment Station, located near the study sites (Berrada et al., 2008)). The field-average volumetric soil moisture was then linearly interpolated between the dates with satellite images to obtain values on every date. The differences between the soil moisture values on adjacent dates provide values for $\Delta\theta$ because Δt was selected to be one day. The treatment of soil moisture in the water balance is highly approximate, but this term makes a small contribution to the overall water balance in Equation (25).

The daily, field-averaged groundwater upflux for both the Manzanola and Swink sites is shown in Figure 14 for a one year period (7/1/07 to 7/1/08). The Rocky Ford site is not considered in this analysis due to its short period of observation. Negative values indicate groundwater recharge from precipitation events, and positive values indicate groundwater upflux. Note the seasonal effect with considerably more upflux occurring during the growing season. This analysis shows that on average 2.3 mm/day of groundwater was lost to ET at the Manzanola site and 2.7 mm/day was lost to ET at the Swink site.

The cumulative ET and G for the Manzanola and Swink study sites are plotted in Figure 15. For the one year period, the cumulative ET was 1.04 m at the Manzanola site and 1.13 m at the Swink site. The total G is estimated to be 0.83 m and 0.97 m at the Manzanola and Swink sites, respectively. These numbers suggest that 80% and 86% of total estimated ET was supplied by groundwater upflux at the Manzanola and Swink sites, respectively. While this calculation relies on several assumptions as described earlier, it suggests that groundwater upflux is the dominant source of water for ET in these fields.
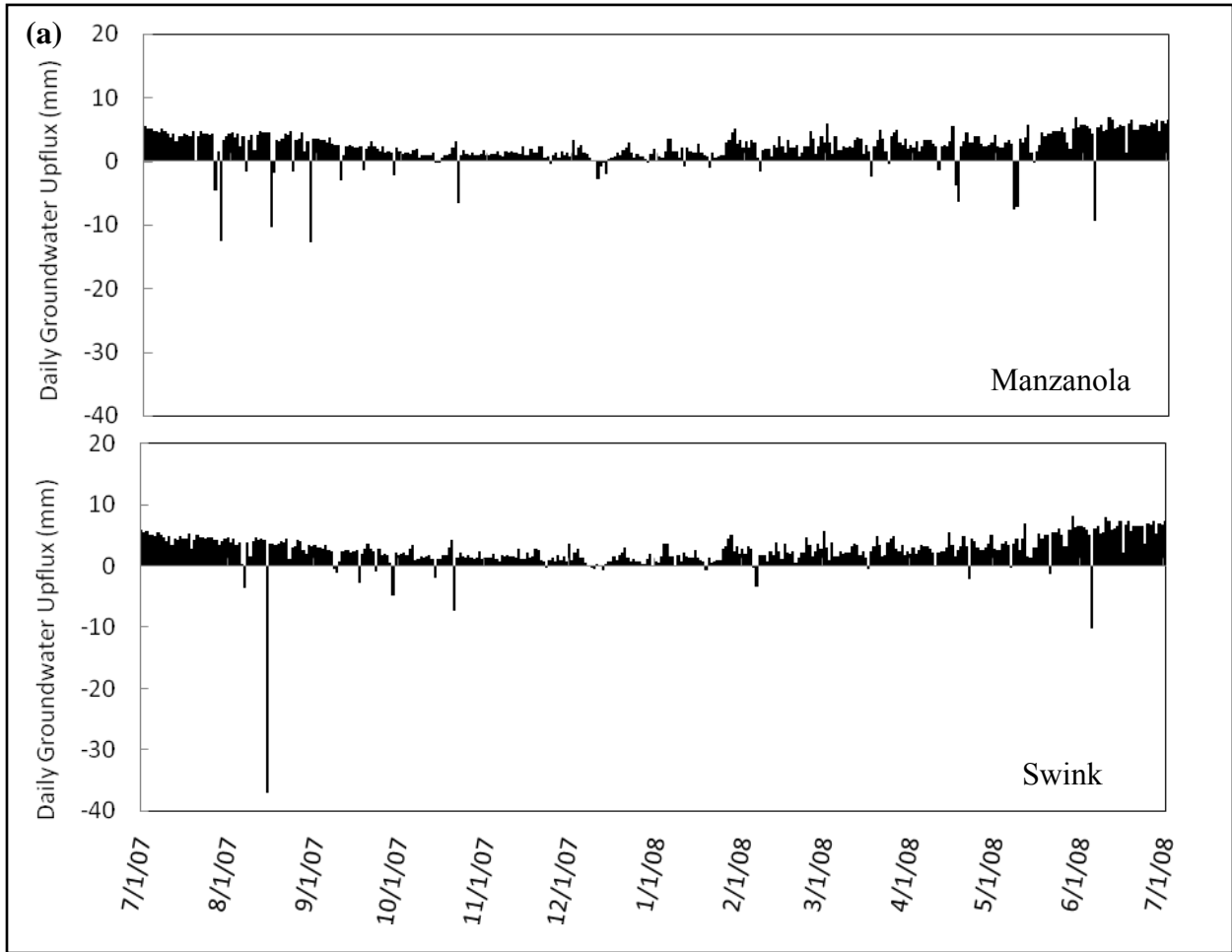
FIGURE 14. *Daily field-averaged groundwater upflux (mm) at (a) the Manzanola site and (b) the Swink site between 7/1/07 and 7/1/08.*
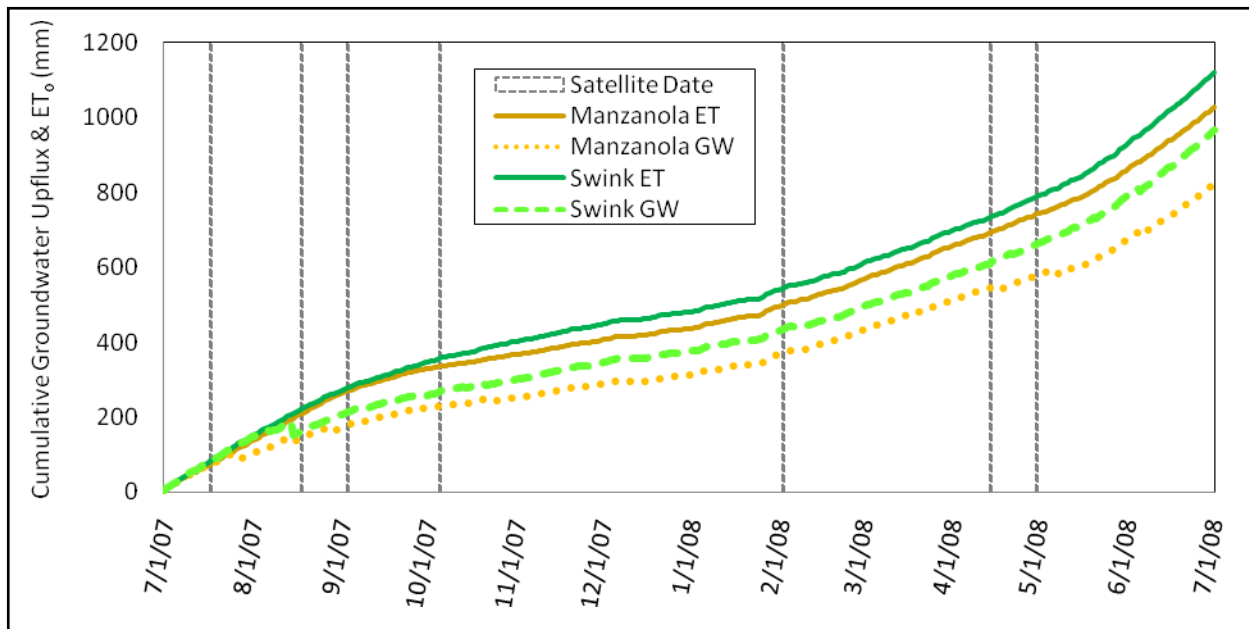
FIGURE 15. *Cumulative ET and groundwater upflux (mm) at the Manzanola and Swink sites between 7/1/07 and 7/1/08. Satellite dates used in water balance calculations are shown as vertical lines.*

Summary and Conclusions

The primary objective of this project was to gain an improved understanding of the relationship between a shallow water table and ET for uncultivated lands in the LARV. Specifically, the project aimed to: (1) determine the factors that control spatial and temporal variations of ET from these uncultivated lands, (2) characterize the dependence of ET on the water table depth, and (3) calculate the portion of ET that is contributed by groundwater upflux. In order to achieve these objectives, three uncultivated field sites in the LARV were monitored in detail from 4/21/07 to 2/28/09. These field sites were named after the nearest town (Manzanola, Rocky Ford, and Swink). ET estimates were obtained at a 30 m x 30 m resolution from a remote sensing method called ReSET that depends on Landsat satellite images. NDVI, which is a measure of vegetation density and greenness, was also obtained from the Landsat images. Reference ET was obtained from a CoAgMet weather station that is near the field sites. Other variables including soil moisture, water table depth, and soil salinity where measured on dates when the satellite passed over the field sites. These measurements were collected at or near a total of 84 monitoring wells that were drilled in support of this study. Precipitation rates and water table depths were also continuously monitored at the field sites using automated instruments.

A regression analysis was performed to determine the factors that control spatial and temporal variations in ET at these sites. In this analysis, a large number of empirical models were calibrated that attempt to explain observed variations in ET using the reference ET and vegetation, soil moisture, groundwater, and soil salinity characteristics. Several variables were considered to represent vegetation influences included NDVI, Julian day of year, and soil temperature. In addition, various functions were considered to describe the influences of soil moisture and water table depth. Overall, the results of this analysis suggest that variations in NDVI are most associated with variations in ET at the field sites. This dependence is logical because vegetation directly performs transpiration. In addition, vegetation patterns also reflect the availability of moisture. In some cases, a function of the Julian day of year, which is

28

associated with vegetation growth and maturity, was the second variable most closely associated with ET variations.

This research also characterized ET's dependence on the water table depth. In the regression analysis, variations in water table depth could explain almost as much of the variation in ET as variations in NDVI. When functions of water table depth are multiplied by the reference ET, they can explain between 65 and 76% of the space-time variation in ET (Table 2). Several equations were considered to model the dependence of ET on water table depth including a linear function, two variations of a power function, and an exponential function (Equations 15-18). All of these functions perform similarly, but the linear function and the exponential function performed slightly better than the power functions. The average ET at each location was also plotted against the average water table depth (Figure 12). This plot indicates that the ET remained quite high even when the water table was relatively deeper (more than 2 m). This result implies that water savings (i.e. reductions in ET) might be difficult to achieve by lowering the water table. In addition, the figure showed that the relationship between ET and water table depth becomes better defined when the data are separated according to their vegetation type (uncultivated alfalfa, grass, and grazed grass). This result suggests that the dependence of ET on water table depth is mediated by vegetation. Thus, future analyses of the water savings that could be achieved by lowering the water table should also consider differences in the vegetation cover and how they might change as the water table is lowered.

Finally, this project calculated the portion of ET that is contributed by groundwater upflux for the field sites. Over a one year period, the cumulative ET was 1.04 m at the Manzanola field site and 1.13 m at the Swink field site. The total groundwater upflux was estimated to be 0.83 m and 0.97 m at the Manzanola and Swink sites, respectively. These numbers imply that on average 2.3 mm/day of groundwater was lost to ET at the Manzanola site and 2.7 mm/day was lost to ET at the Swink site. They also suggest that 80% and 86% of total estimated ET was supplied by groundwater upflux at the Manzanola and Swink sites, respectively. Thus, upflux from groundwater is the dominate source for ET at these uncultivated field sites.

Future research should consider field sites with deeper water tables to determine whether high ET rates continue when the water table is very low. Such field sites might also allow a better determination of the functional dependence of ET on water table depth. Future research should also consider the role of vegetation patterns and changes in more detail. In particular, when the water table is lowered, the succession of vegetation should be documented to determine how quickly plants with deeper roots take hold and how efficient those plants are at maintaining the high level of ET. This issue could be analyzed by studying the ET, water table depth, and vegetation of a retired field over a prolonged period of time.

In summary, this project demonstrated that upflux from shallow groundwater under uncultivated lands in the LARV is a significant portion of the water balance for these areas. Because uncultivated lands represent a significant portion of the irrigated river valley and shallow water tables are likely to underlay a significant portion of these lands, this project hints that such upflux is also a major contribution to the overall water balance of the valley. This upflux needs to be carefully considered in regional hydrologic modeling and water management. The study also shows that the ET rate remains high even when the water table is relatively deep. This suggests that the upflux is relatively robust to changes in the water table and that water savings may be difficult to achieve by lowering the water table. However, even the small changes in ET observed for these fields may become significant when applied over a regional scale.

References

Albertson, J. D., and Kiely, G. (2001). "On the structure of soil moisture time series in the context of land surface models." *Journal of Hydrology*, 243(1-2), 101-119.

Allen, R. G., Pereira, L. S., Raes, D., and Smith, M. (1998). "Crop evapotranspiration - guidelines for computing crop water requirements." Food and Agriculture Organization of the United Nations, Rome.

Asrar, G., Fuchs, M., Kanemasu, E. T., and Hatfield, J. L. (1984). "Estimating absorbed photosynthetically radiation and leaf area index from spectral reflectance in wheat." *Agronomy Journal*, 76, 300-306.

Bastiaanssen, W. G. M., Menenti, M., Feddes, R. A., and Holtslag, A. A. M. (1998). "A remote sensing surface energy balance algorithm for land (SEBAL). 1. Formulation." *Journal of Hydrology*, 212, 198-212.

Berrada, A., Hooten, T.M., Cardon, G.E., Broner, I. (2001). "Assessment of irrigation water management and demonstration of irrigation scheduling tools in the full service area of the Dolores project: 1996-2000 Part II: Calibration of the Watermark soil moisture sensor and ETgage atmometer." Colorado State University.

Berrada, A., Hooten, T.M., Cardon, G.E., Broner, I., Simmons, L., Straw, D., Bartolo, M., and Ley, T. (2008). "The large lysimeter at the Arkansas Valley Research Center: objectives and accomplishments." Colorado State University.

Burkhalter, J. P., and Gates, T. K. (2005). "Agroecological impacts from salinization and waterlogging in an irrigated river valley." *Journal of Irrigation and Drainage Engineering*, 131(2), 197-209.

Burkhalter, J. P., and Gates, T. K. (2006). "Evaluating regional solutions to salinization and waterlogging in an irrigated River Valley." *Journal of Irrigation and Drainage Engineering*, 132(1), 21-30.

Colorado Climate Center. (2008). "Colorado Climate Center, 2008, CoAgMet Homepage."

Cooper, D. J., Sanderson, J. S., Stannard, D. I., and Groeneveld, D. P. (2006). "Effects of long-term water table drawdown on evapotranspiration and vegetation in an arid region phreatophyte community." *Journal of Hydrology*, 325(1-4), 21-34.

Elhaddad, A., and Garcia, L. A. (2008). "Surface energy balance-based model for estimating evapotranspiration taking into account spatial variability in weather." *ASCE Journal of Irrigation and Drainage* In Press.

Emery, P. A. (1973). "Water in the San Luis Valley, South-Central Colorado." Colorado Water Conservation Board, Denver.

Emery, P. A. (1991). "Testimony in Case No. 86CW46, District Court, Water Division No. 3, State of Colorado." Transcript page 5741.

Gamon, J. A., Field, C. B., Goulden, M. L., Griffen, K. L., Hartley, A. E., Geeske, J., Penuelas, J., and Valentini, R. (1995). "Relationships between NDVI, canopy structure, and photosynthesis in three Californian vegetation types." *Ecological Applications*, 5(1), 28-41.

Gates, T. K., Garcia, L. A., and Labadie, J. W. (2006). "Toward optimal water management in Colorado's Lower Arkanasas River Valley: monitoring and modeling to enhance agriculture and environment."

Gavlak, R., Hornbeck, D., Miller, R., and Kotuby-Amacher, J. (2003). Soil, plant, and water reference methods for the western states region. WCC-103 Publication, WREP-125.

Gowing, J. W., Konukcu, F., and Rose, D. A. (2006). "Evaporative flux from a shallow watertable: The influence of a vapor-liquid phase transition." *Journal of Hydrology*, 321(1-4), 77-89.

Groeneveld, D. P., Baugh, W. M., Sanderson, J. S., and Cooper, D. J. (2007). "Annual groundwater evapotranspiration mapped from single satellite scenes." *Journal of Hydrology*, 344(1-2), 146-156.

Herting, A. W., and Gates, T. K. (2006). "Assessing and modeling irrigation-induced selenium in the stream-aquifer system of the Lower Arkansas River Valley, Colorado." Colorado State University Hydrology Days, Colorado State University, Fort Collins, Colorado.

Huntley, D. (1979). "Ground-water recharge to the aquifers of Northern San Luis Valley."

Nakano, T., Nemoto, M., and Shinoda, M. (In Press). "Environmental controls on photosynthetic production and ecosystem respiration in semi-arid grasslands of Mongolia." *Agricultural and Forest Meteorology*, In Press, Corrected Proof.

Nichols, W. D. (1994). "Groundwater discharge by phreatophyte shrubs in the Great Basin as related to depth to groundwater." *American Geophysical Union in Water Resources Research*, 30(12), 3265-3274.

Nichols, W. D. (2000). "Regional groundwater evapotranspiration and groundwater budgets, Great Basin Nevada."

Pikul, J. L. (2008). "Soil water measurement: gravimetric." *Encyclopedia of Water Science, Second Edition*, 1:1, 1063 - 1065.

Sanderson, J. S., and Cooper, D. J. (2008). "Ground water discharge by evapotranspiration in wetlands of an arid intermountain basin." *Journal of Hydrology*, 351(3-4), 344-359.

Snyder, R. L., Eching, S. (2002). "Penman-Monteith daily (24-hour) Reference Evapotranspiration Equations for Estimating ET_o, ET_r and HS ET_o with Daily Data." Regents of the University of California

Susfalk, R., Dada, D., Martin, C., Young, M., Gates, T., Rosamond, C., Mihevc, T., Arrowood, T., Shanafield, M., Epstein, B., Fitzgerald, B., Lutz, A., Woodrow, J., Miller, G., and Smith, D. (2008). "Evaluation of linear anionic polyacrylamide (LA-PAM) application to water delivery canals for seepage reduction." Technical Report for the U.S. Bureau of Reclamation.

Teuling, A. J., and Troch, P. A. (2005). "Improved understanding of soil moisture variability dynamics." *Geophys. Res. Lett*, 32(5).

Torres, J. S., and Hanks, R. J. (1989). "Modeling water table contribution to crop evapotranspiration." *Irrigation Science*, 10, 265-279.

Tucker, C. J. (1979). "Red and photographic infrared linear combinations for monitoring vegetation." *Remote Sensing of Environment*, 8, 127-150.

Wichelns, D. (1999). "An economic model of waterlogging and salinization in arid regions." *Ecological Economics*, 30(3), 475-491.

Wittler, J. M., Cardon, G. E., Gates, T. K., M.ASCE, Cooper, C. A., and Sutherland, P. L. (2006). "Calibration of Electromagnetic Induction for Regional Assessment of Soil Water Salinity in and Irrigated Valley." *Journal of Irrigation and Drainage Engineering*, 132, 436-444.

Yan, W., and Wallace, D. H. (1998). "Simulation and Prediction of Plant Phenology for Five Crops Based on Photoperiod×Temperature Interaction." *Annals of Botany*, 81(6), 705-716.

Young, C., Wallender, W., Schoups, G., Fogg, G., Hanson, B., Harter, T., Hopmans, J., Howitt, R., Hsiao, T., Panday, S., Tanji, K., Ustin, S., and Ward, K. (2007). "Modeling Shallow Water Table Evaporation in Irrigated Regions." *Irrigation Drainage Systems*, 21(2), 119-132.